Common Mechanisms of DNA translocation motors in Bacteria and Viruses Using One-way Revolution Mechanism without Rotation

Peixuan Guo,[1]* Zhengyi Zhao,[1] Jeannie Haak,[1] Shaoying Wang,[1] Dong Wu[2], Bing Meng[3] and Tao Weitao[4]

[1]Nanobiotechnology Center, Markey Cancer Center, and College of Pharmacy, University of Kentucky, Lexington, KY, 40536, USA; [2]iHuman Institute, Shanghai Tech University, Shanghai 201210, China; [3]National Lab of Biomacromolecules, Institute of Biophysics, Chinese Academy of Sciences, Beijing 100101, China; [4]Biology Department, College of Science and Mathematics, Southwest Baptist University, Bolivar, Missouri, 65613, USA

Article Info

Keywords:

Bionanomotor,

One-way traffic mechanism,

DNA packaging,

Virus assembly,

Bionanotechnology,

Binary fission,

Chromosome segregation,

DNA repair,

Holliday junction,

Homologous recombination

Abstract

Biomotors were once described into two categories: linear motor and rotation motor. Recently, a third type of biomotor with revolution mechanism without rotation has been discovered. By analogy, rotation resembles the Earth rotating on its axis in a complete cycle every 24 h, while revolution resembles the Earth revolving around the Sun one circle per 365 days (see animations http://nanobio.uky.edu/movie.html). The action of revolution that enables a motor free of coiling and torque has solved many puzzles and debates that have occurred throughout the history of viral DNA packaging motor studies. It also settles the discrepancies concerning the structure, stoichiometry, and functioning of DNA translocation motors. This review uses bacteriophages Phi29, HK97, SPP1, P22, T4, and T7 as well as bacterial DNA translocase FtsK and SpoIIIE or the large eukaryotic dsDNA viruses such as mimivirus and vaccinia virus as examples to elucidate the puzzles. These motors use ATPase, some of which have been confirmed to be a hexamer, to revolve around the dsDNA sequentially. ATP binding induces conformational change and possibly an entropy alteration in ATPase to a high affinity toward dsDNA; but ATP hydrolysis triggers another entropic and conformational change in ATPase to a low affinity for DNA, by which dsDNA is pushed toward an adjacent ATPase subunit. The rotation and revolution mechanisms can be distinguished by the size of channel: the channels of rotation motors are equal to or smaller than 2 nm, that is the size of dsDNA, whereas channels of revolution motors are larger than 3 nm. Rotation motors use parallel threads to operate with a right-handed channel, while revolution motors use a left-handed channel to drive the right-handed DNA in an anti-chiral arrangement. Coordination of several vector factors in the same direction makes viral DNA-packaging motors unusually powerful and effective. Revolution mechanism that avoids DNA coiling in translocating the lengthy genomic dsDNA helix could be advantageous for cell replication such as bacterial binary fission and cell mitosis without the need for topoisomerase or helicase to consume additional energy.

*Address correspondence: Peixuan Guo, Ph. D. William Farish Endowed Chair in Nanobiotechnology, College of Pharmacy, University of Kentucky, 565 Biopharm Complex, 789 S. Limestone Str, Lexington, KY 40536, Email: peixuan.guo@uky.edu, Phone: (859) 218-0128 (office).

1. Introduction

For decades, the popular viral DNA-packaging motor (Fig. 1) has been believed to be a rotation motor with double-stranded (ds) DNA serving as a bolt and the protein channel as a nut (Hendrix,1978.). The finding of the twisting and twirling of the motor channel structure, as revealed by crystal studies of biomotors (Guasch et al.,2002.; Simpson et al.,2001.), has reinforced the popular notion of a rotation mechanism in the scientific community. However, if the DNA packaging motor (Fig. 1) were considered to be a rotation machine, either the motor or the DNA would have to rotate during dsDNA advancing. But extensive studies have revealed that neither the channel nor the dsDNA rotates during transportation. When the connector and the procapsid protein were fused to each other and the rotation of the connector within the procapsid was not possible, the motors were still active in packaging, implying that connector rotation is not necessary for DNA packaging (Baumann et al.,2006.; Maluf and Feiss,2006.). Studies using single-molecule force spectroscopy combined with polarization spectroscopy have also indicated that the connector did not rotate (Hugel et al.,2007.).

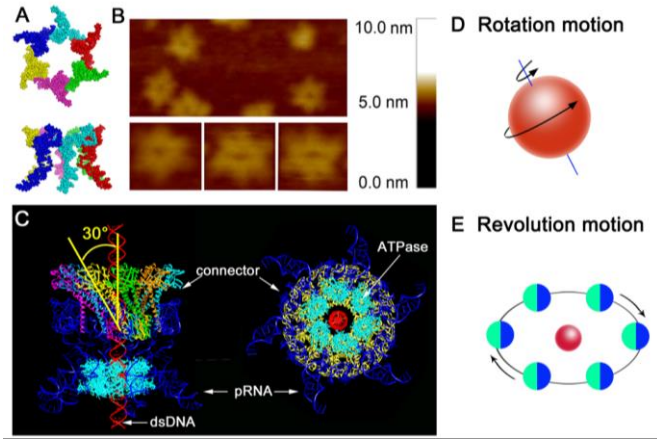

Fig. 1. Depiction of the structure and function of phi29 DNA packaging motor. A. Crystal structure of hexameric pRNA (adapted from Zhang et al., 2013 with permission of Cold Spring Harbor Laboratory Press). B. AFM images of loop-extended hexameric pRNA. C. Illustrations of the phi29 DNA packaging motor in side view (left) and bottom view (right) (B and C adapted from Schwartz et al., 2013a with permission of Elsevier). D and E. Illustration of the rotation and revolution motions (for animation, please see http://nanobio.uky.edu/Connector-DNA_revolution.wmv). (adapted from De-Donatis et al., 2014) with permission from BioMed Central.

Tethering of DNA ends to bead clusters demonstrated that DNA translocation by the motor was still active, and no rotation of the beads was observed either (Chang et al.,2008.; Shu et al.,2007.) (Fig. 2). The possibility of having bead rotation undetectable due to bond freedom between bead and dsDNA was excluded by applying bead clusters (Chang et al.,2008.; De-Donatis et al.,2014.).

Many mysteries have since been encountered in the course of the study of dsDNA translocation motors (Chen and Guo,1997b.; Grimes and Anderson,1997.; Guo et al.,1998.; Hendrix,1978.; Moffitt et al.,2009.; Serwer,2003.; Serwer,2010.). Many thorough reviews on the packaging of dsDNA viruses are available (Casjens,2011.; Guo and Lee,2007.; Lee et al.,2009.; Sun et al.,2010.; Yu et al.,2010.). Tetrameric, pentameric and hexameric motor models have been proposed for the motor structures and motor mechanisms (Guo et al.,1998.; Moffitt et al.,2009.; Ortega and Catalano,2006.; Shu et al.,2007.; Sun et al.,2007.). Recently, a third type of biomotor has been discovered in the phi29 DNA packaging motor that exercise a revolution mechanism without rotation (Fig. 1) (for animation see http://nanobio.uky.edu/movie.html). The finding has solved many mysteries and puzzles. This review intends to address specifically the revolution mechanism and how this finding reconciles the data reported during the last 35 years, how the motor transports close circular dsDNA without breaking any covalent-bonds or changing the DNA topology, and how the motor controls a one-way DNA movement despite the intrinsic bidirectional nature of the dsDNA helix. The above conjectures have been tested and verified with detection of a novel revolution instead of rotation mechanism.

2. The ASCE biomotors including the AAA+ and FtsK-HerA superfamilies display a hexameric arrangement

It has been a long and fervent debate over whether the DNA packaging motor of dsDNA viruses contains six or five copies of components to drive the motor. Viral structure studies reveal that viral icosahedron capsid is composed of many pentamers and hexamers (Caspar and Klug,1962.). It has been found that the DNA packaging motor of dsDNA viruses resides within the pentameric vertex (Bazinet and King,1985.). Since the motor channel for dsDNA bacteriophages is a dodecamer (Agirrezabala et al.,2005.; Cardarelli et al.,2010.; Carrascosa et al.,1982.; Doan and Dokland,2007.; Kochan et al.,1984.; Valpuesta et al.,1992.), this 12-fold symmetry can be interpreted as a hexamer of dimers. Such special structural

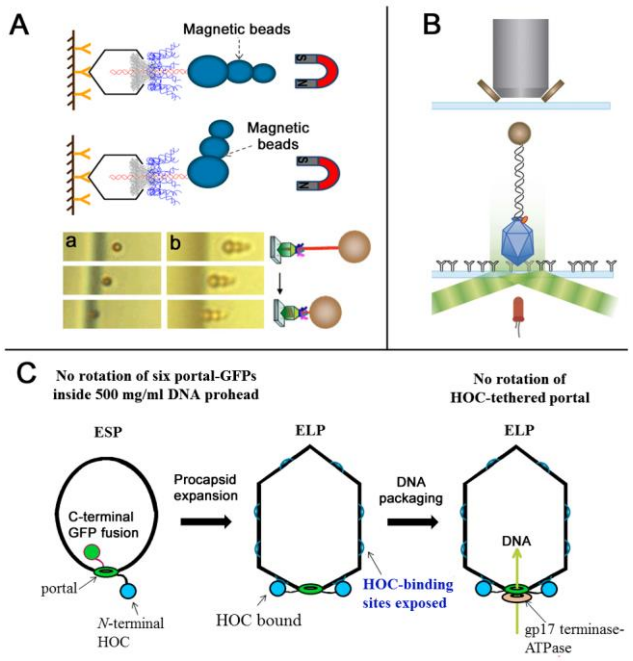

Fig. 2. Experiment of T4 and phi29 motor revealing that neither connector nor dsDNA rotation is required for active DNA packaging. A. Direct observation of DNA packaging horizontally using a dsDNA with its end linked to a cluster of magnetic beads for stretching the DNA. "a" and "b" are real-time sequential images of DNA-magnetic bead complexes (adapted from Chang et al., 2008 with permission from the AIP publishing group). B. Schematic of the single molecule experimental geometry of phi29 DNA packaging motor to show no rotation of the connector during DNA packaging (adapted from Hugel et al., 2007). C. Experiment revealing that T4motor connector does not rotate during packaging. The packaging activity is not inhibited with N-terminal of motor connector protein fused and tethered to its protease immune binding site on capsid (adapted from Baumann et al., 2006 with permission from John Wiley and Sons).

arrangement has, since 1978, led to the popularity of a novel rotation motor with a five-fold/six-fold mismatch gearing mechanism (Hendrix,1978.). Recent publications of the hexameric pRNA crystal structure (Zhang et al.,2013.), the AFM images of the hexameric pRNA ring (Shu et al.,2013a.; Shu et al.,2013b.; Zhang et al.,2013.), and the finding of hexameric ATPase gp16 (Schwartz et al.,2013a.), have excluded the pentamer speculation. Nevertheless, finding of the revolution mechanism without rotation (Guo et al.,2013b.; Schwartz et al.,2013b.; Schwartz et al.,2013a.; Zhao et al.,2013.) helps resolve and conciliate the hexamer and pentamer discrepancy, since motors

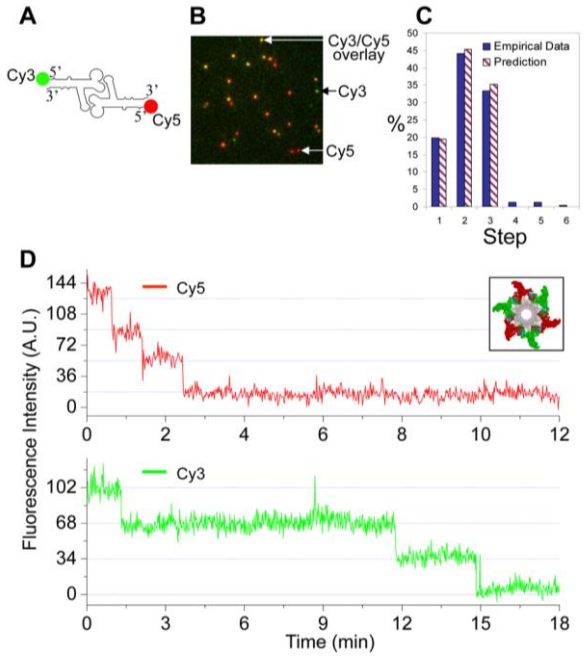

Fig. 3. Single molecule photo-bleaching and confirmation of the presence of six copies of phi29 motor pRNA via dual-viewimaging of procapsids containing three copies of Cy3-pRNA and three copies of Cy5-pRNA. A. pRNA dimer design constructed with Cy3- and Cy5-pRNA. B. Typical fluorescence image of procapsids with dual-labeled pRNA dimers showing the labeled Cy3 (green), Cy5 (red) and both (yellow). C. Comparison of empirical photobleaching steps with theoretical prediction of Cy3-pRNA in procapsids bound with dual-labeled dimers. D. Photobleaching steps of procapsids reconstituted with the dimer (adapted from Shu et al., 2007 with permission from John Wiley and Sons).

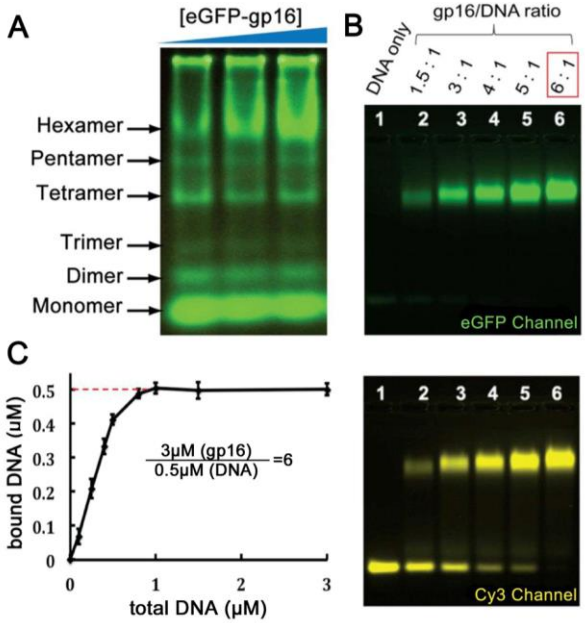

Fig. 4. Stoichiometric assays showing the formation of the hexamer of phi29motor ATPase gp16. A. Native gel revealed six distinct bands characteristic of the six oligomeric states of the ATPase; the hexamer increased as the concentration of protein increased. B. Slab gel showing the binding of ATPase to dsDNA in a 6:1 ratio; imaged in GFP (upper) and Cy3 channels (lower) for ATPase and dsDNA, respectively. C. Quantification by varying the molar ratio of [ATPase]:[DNA]. The concentration of bound DNA plateaus at a molar ratio of 6:1 (adapted from Schwartz et al., 2013a with permission from the Elsevier).

with any subunit stoichiometry can utilize the revolution mechanism. However, the use of a revolution mechanism by a hexamer motor has raised a striking question: Why do most ASCE (additional strand catalytic E) biomotors including the AAA+ (ATPases Associated with diverse cellular Activities) and FtsK-HerA superfamilies display a hexameric but not pentameric arrangement?

One fundamental process of all living organisms is to transport dsDNA. The ASCE superfamily including the AAA+ and FtsK-HerA superfamilies, is a clade of nanomotors that facilitates a wide range of functions (Ammelburg et al.,2006.; Guo and Lee,2007.; Snider et al.,2008.; Snider and Houry,2008.), many of which are involved in dsDNA riding, tracking, packaging, and translocation. These functions are critical to DNA repair, replication, recombination, chromosome segregation, DNA/RNA transportation, membrane sorting, cellular reorganization, cell division, bacterial binary fission, and many other processes (Ammelburg et al.,2006.; Martin et al.,2005.). This family can convert energy from ATP into a mechanical motion (Chemla et al., 157 2005; Guo et al., 1987c; Hwang et al., 1996; Sabanayagam et al., 2007; 158 Schwartz et al., 2012).. This usually involves the conformational changes of an ATPase enzyme (Guenther et al.,1997.; McNally et al.,2010.). The feature of these nanomotors is the hexameric arrangement that members of this family often display (Aker et al.,2007.; Chen et al.,2002.; Mueller-Cajar et al.,2011.; Wang et al.,2011.; Willows et al.,2004.). The hexamer arrangement facilitates bottom-up assembly in nanomachine manufacturing and produce stable structure engagements and robust machines that can be artfully functionalized in human cells to remedy functional defects.

Different models have been proposed for the motor of dsDNA viruses (Aathavan et al.,2009.; Guo and Lee,2007.; Moffitt et al.,2009.; Serwer,2010.; Yu et al.,2010.; Zhang et al.,2012.). Until recently, it has been believed that they contain a five-fold/six-fold mismatch structure (Hendrix,1978.). In 1986, the phi29 DNA packaging motor was constructed *in vitro* (Guo et al.,1986.), and has been found to have three co-axial rings: pRNA, connector, and gp16 ATPase ring (Fujisawa et al., 1991.; Guo et al.,1987a.; Ibarra et al.,2001.; Lee and Guo,2006.) (Fig. 1). In 1998, the pRNA ring was determined to exist as a hexameric ring (Guo et al.,1998.; Zhang et al.,1998.) (featured by *Cell* (Hendrix,1998.)). In 2000, it was verified by Cryo-electron microscopy (Cryo-EM) to be hexameric in shape (Ibarra B et al.,2000.). But studies by others have put forward a pentameric model (Chistol et al.,2012.; Morais et al.,2008.; Yu et al.,2010.). However, biochemical analysis (Guo et al.,1998.; Hendrix,1998.; Zhang et al.,1998.), single molecule photobleaching study (Shu et al.,2007.), gold labeling imaging by electron microscopy (EM) (Moll and Guo,2007.; Xiao et al.,2008.), and RNA crystal structure studies (Zhang et al.,2013.) have all revealed hexameric assembly of pRNA. One interesting theory has been proposed that the motor initially assembles as a hexamer but one of the subunits departs before DNA packaging starts, thus generating a pentamer (Morais et al.,2001.; Morais et al.,2008.; Simpson et al.,2000.). However, single molecule photobleaching analysis of DNA-packaging intermediates showed that the active motor still contained six copies of pRNA during DNA translocation (Shu et al.,2007.) (Fig. 3), and pRNA dimers were the building blocks for hexameric ring, which is assembled through the pathway of 2 → 4 → 6 pRNAs.

The formation of gp16 into an active hexameric complex in the phi29 DNA packaging has been further demonstrated by using a Walker B mutant gp16 that could bind but not hydrolyze ATP, as the activity of the assembly containing a different number of mutant monomers followed a binomial distribution model (Chen et al.,1997.; Schwartz et al.,2013a.; Trottier and Guo,1997.). Empirical results have been obtained in conjunction with stoichiometric data to show that the motor complex is hexameric (Schwartz et al.,2013a.). Moreover, qualitative DNA binding assays, capillary electrophoresis assays (CE), and electrophoretic mobility shift assays (EMSA) have

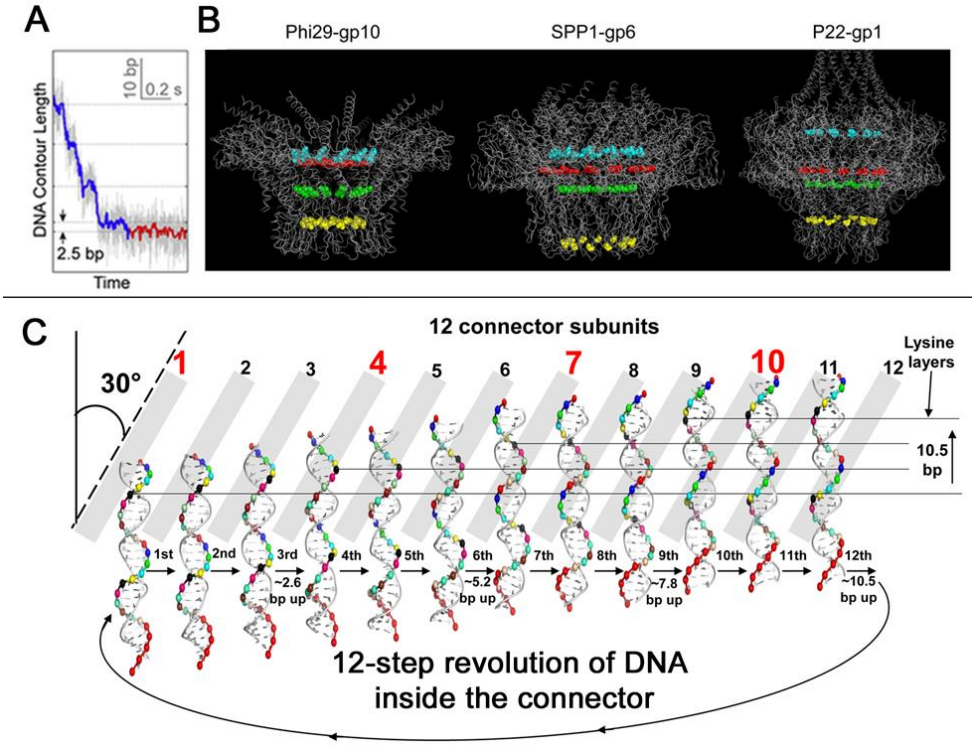

Fig. 5. Experiment and the proposed mechanismrevealing four steps of pauses for each circle during the packaging of phi29 dsDNA via electrostatic interaction. A. Sample packaging traces showing four pauses during dsDNA advancing (adapted fromChistol et al., 2012 with permission of the Elsevier). B. The presence of four lysine residues ofmotor channel protein leads to the formation of four positively charged rings in different motors (PDB IDs: Phi29-gp10, 1H5W. (Guasch et al., 2002); SPP1-gp6, 2JES. (Lebedev et al., 2007); P22-gp1, 3LJ5. (Olia et al., 2011)) (adapted fromFang et al., 2012with permission fromElsevier). C. Diagramshowing DNA revolution inside phi29 connector channel with four steps of pause due to the interaction of four positively charged lysine rings with the negatively charged dsDNA phosphate backbone. DNA revolution across the 12 connector channel subunits is shown. The uneven electrical static interaction resulting from themis-gearing between 10.5-base pairs per DNA helical turn and 12 subunit per round of the channel is the cause leading to the observation of uneven steps (adapted with permission from (Zhao et al., 2013). Copyright (2013) American Chemical Society).

demonstrated that the final oligomeric state of ATPase is hexamer (Schwartz et al.,2013a.) (Fig. 4).

There has been be some discrepancies over the motor stoichiometries and the mechanisms. A compression mechanism found in the T4 DNA packaging motor (Dixit et al.,2012.; Ray et al.,2010.) supports the revolution mechanism but disagrees with the pentamer gp17 model of T4. This compression mechanism also supports the revolution mechanism and the "Push through a One-Way Valve" model, as previously described (Guo and Lee,2007.; Jing et al.,2010.; Zhang et al.,2012.; Zhao et al.,2013.). There seems to be another discrepancy over the pentamer model of the phi29 motor, as other studies have demonstrated four steps, instead of five, of motor action, as revealed by laser trap experiments (Fig. 5A). To reconcile these discrepancies, the group proposed a model in which one of the subunits in the pentamer ring is inactive, and the other four subunits are active during the DNA packaging process (Moffitt et al.,2009.; Yu et al.,2010.). These four steps have been recently shown to be a result of the four relaying lysine layers embedded inside the phi29 connector channel inner wall (Fig. 5B, 5C) (Zhao et al.,2013.), further disproving the pentamer model (see section of electrostatic interaction).

3. A motor with a revolution rather than rotation mechanism in dsDNA translocation has been discovered in bacteriophage phi29

Viral dsDNA packaging motors consist of a protein channel and two packaging components to carry out activities of viral DNA packaging (Fig. 1), the larger one is an ATPase, and the smaller one is for dsDNA binding (Guo et al.,1987c.; Guo et al.,1998.). This notion has now been popularly acknowledged. The motor connector

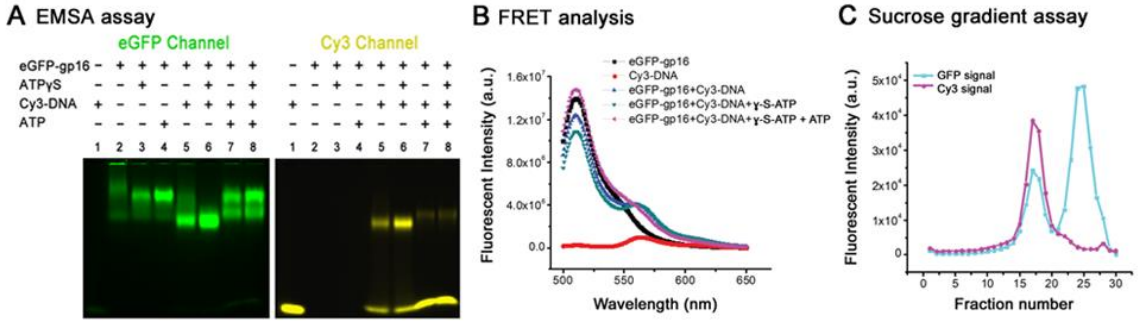

Fig. 6. Various approaches showing the binding of dsDNA with the ATPase under different conditions, revealing the different conformations and different dsDNA affinities of the ATPase upon ATP binding and hydrolysis. A. EMSA assay (adapted from Schwartz et al., 2013a with the permission of Elsevier). B. FRET analysis. C. Sucrose gradient assay (B and C adapted from Schwartz et al., 2012 with permission from Oxford University Press).

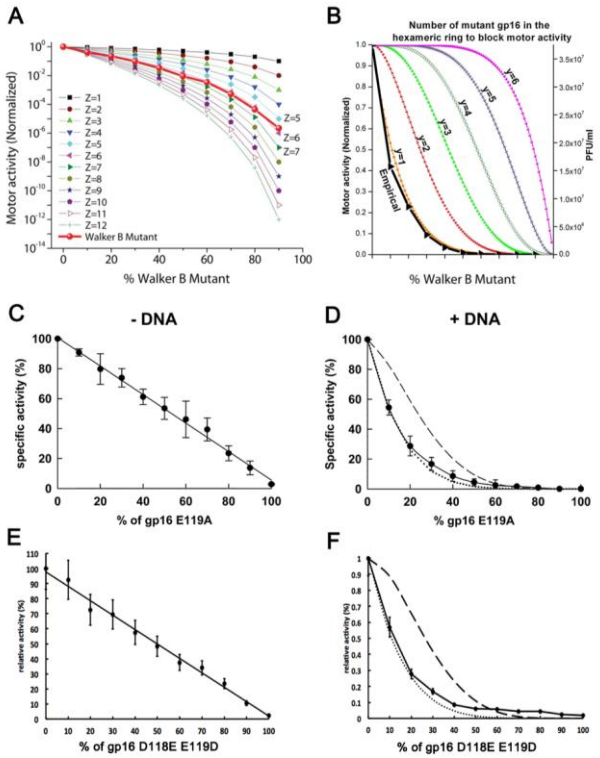

Fig. 7. Inhibition assays revealing stoichiometry of motor components and cooperativity of motor subunits. A. Binomial distribution assay reveals that the ATPase gp16 ring have six copies (highlighted) in the DNA packaging motor (adapted from Schwartz et al., 2013a with the permission of Elsevier). B. Binomial distribution assay demonstrating one inactive Walker B ATPase mutant subunit within the hexamer blocked motor activity. C. The inhibition ability of inactive Walker B mutants in the absence (C, E) and presence (D, F) of dsDNA reveals cooperativity of motor subunits, supporting the sequential action and revolution mechanism (adapted from Schwartz et al., 2013b with the permission of Elsevier).

contains a center channel encircled by 12 copies of the protein gp10 that serves as a pathway for dsDNA translocation (Guasch et al.,2002.; Jimenez et al.,1986.).

Besides the well-characterized connector channel core, the motor of bacterial Phi29 also contains a hexameric packaging RNA ring (Guo et al.,1987a.; Guo et al.,1998.; Shu et al.,2007.; Zhang et al.,2013.) (Fig. 1). During packaging, ATP binds to one ATPase subunit and stimulates ATPase to adapt a new conformation, with a conformational entropy alteration (De-Donatis et al.,2014.), resulting in a higher affinity to dsDNA. Upon ATP hydrolysis, the ATPase gp16 (Grimes and Anderson,1990.; Guo et al.,1987b.; Guo et al.,1987c.; Ibarra et al.,2001.; Lee and Guo,2006.; Lee et al.,2008.) assumes a new conformation, and another conformational entropy resume, resulting in a lower affinity to dsDNA, thus pushing dsDNA away from the subunit and transferring it to an adjacent subunit by a power stroke (Fig. 6) (Schwartz et al.,2012.; Schwartz et al.,2013b.; Schwartz et al.,2013a.). EMSAs have shown that the motor ATPase gp16's affinity towards dsDNA increases in the presence of ATPγs (Fig. 6), but remains low in the presence of ADP, AMP, or in the absence of nucleotide (Schwartz et al.,2012.). Cooperativity and sequential action among the ATPase subunits also promote the revolution of dsDNA along the connector channel (Chen and Guo,1997a.; Moffitt et al.,2009.), as determined by Hill constant and binomial behavior of the activity in the inhibition assays due to incorporation of mutant subunits (Fig. 7). The DNA revolves unidirectionally along the hexameric channel wall, but neither the dsDNA nor the hexameric ring rotates (Schwartz et al.,2013b.; Zhao et al.,2013.) (Fig. 8). One ATP is hydrolyzed in each transitional step and six ATPs are consumed in one cycle to translocate the dsDNA one helical turn of 360° (Schwartz et al.,2012.; Schwartz et al.,2013b.). The binding of ATPase on the channel wall along the same phosphate backbone chain, but at a location 60° different from the last contact, drives dsDNA forward 1.75 bp each step (10.5 bp/turn ÷ 6 ATP = 1.75 bp/ATP) and revolves it without any rotation of the ATPase or dsDNA (Schwartz et al.,2013b.; Zhao et al.,2013.) (Fig. 9).

An anti-chiral arrangement (an opposite handedness) exists between the dsDNA helix and the channel subunits of the connector dodecamer, as revealed by crystallography (Guasch et al.,2002.; Simpson et al.,2001.). The connector helix has 12 subunits that display a tilt of 30°. Since one turn of the helix of dsDNA advances 360°, the dsDNA shifts 30° every time it passes one of the 12 subunits (360° ÷ 12 = 30°), and the angle is compensated for by the 30° tilting of the subunit of channel wall (Fig. 1C), resulting in the transportation of the helices without rotation, coiling, or a torsion force. The contact between the connector and the dsDNA chain is transferred from one point on the phosphate backbone to another along one strand in a 5' to 3' direction (Moffitt et al.,2009.; Schwartz et al.,2013b.; Zhao et al.,2013.).

An effective mechanism of coordination between gp16 and dsDNA operates by using the ATP hydrolysis cycle as means of regulation. Motor ATPase tightly clinches dsDNA after binding to ATP and subsequently pushes the dsDNA away after ATP hydrolysis. Only one molecule of ATP is sufficient to generate the high affinity state for DNA in the ring of the motor ATPase. The mixed oligomers of the wild type and the mutants display a negative cooperativity and a communication between the subunits of gp16 oligomer (Schwartz et al.,2012.; Schwartz et al.,2013b.; Schwartz et al.,2013a.). In the presence of dsDNA, a rearrangement occurs within the subunits of gp16 that enables them to communicate between each other and to "sense" the nucleotide state of the reciprocal subunit. This observation supports that only the subunit that binds to the substrate at any given time is permitted to hydrolyse ATP, thus performing translocation while the other subunits are in the "stalled" or "loaded" state. This suggests an extremely high level of coordination on the function of the protein, likely the most efficient process to couple energy production with DNA translocation *via* ATP hydrolysis among the biomotors studied so far (Fig. 9).

More recently, Kumar and Grubmuller reported their studies on the physical and structural properly of the connecter of phi29 DNA packaging motor (Kumar and Grubmuller, 2014 in press; see also the Commentary by Guo, 2014 in press). Their newevidence based on independent biophysical studies supports the one-way revolution mechanism of biomotors. Using dynamic simulations, the elasticity and stiffness of connector channel was probed down to the atomic level. The author used their biophysical data to rule out untwist–twist DNA packaging model (Simpson et al., 2000) proposed previously. Their equilibrium and nonequilibrium force probe *via* MD simulations revealed that the connector as a whole is softer than the procapsid, yet the central region of the connector is one of the most rigid proteins known. Their calculation revealed that the previously proposed 12° untwisting requires ten times more energy (Kumar and Grubmuller, 2014 in press). Moreover, the umbrella sampling simulations suggest that 100 kJ/mol is required for only a 4° untwisting of the entire connector. Kumar and Grubmuller's data also demonstrates why the connector is able to withstand a large pressure variation of up to ~60 atm. With data together made them conclude that the overall connector's mechanical properties aligns well with the newly reported one-way revolution model (Schwartz et al., 2012, 2013a, 2013b). The authors pointed out that the connector as a one-way valve preventing reversal of DNA from the procapsid during packaging and the inner flexible connector loop serves as a check-valve (Fang et al., 2012; Zhang et al., 2012; Zhao et al., 2013). The value of these conclusions is, not only in the solid data, but also in the authors' rational interpretation of the mechanism following data acquisition. They did not simply follow the idea in literature; instead,

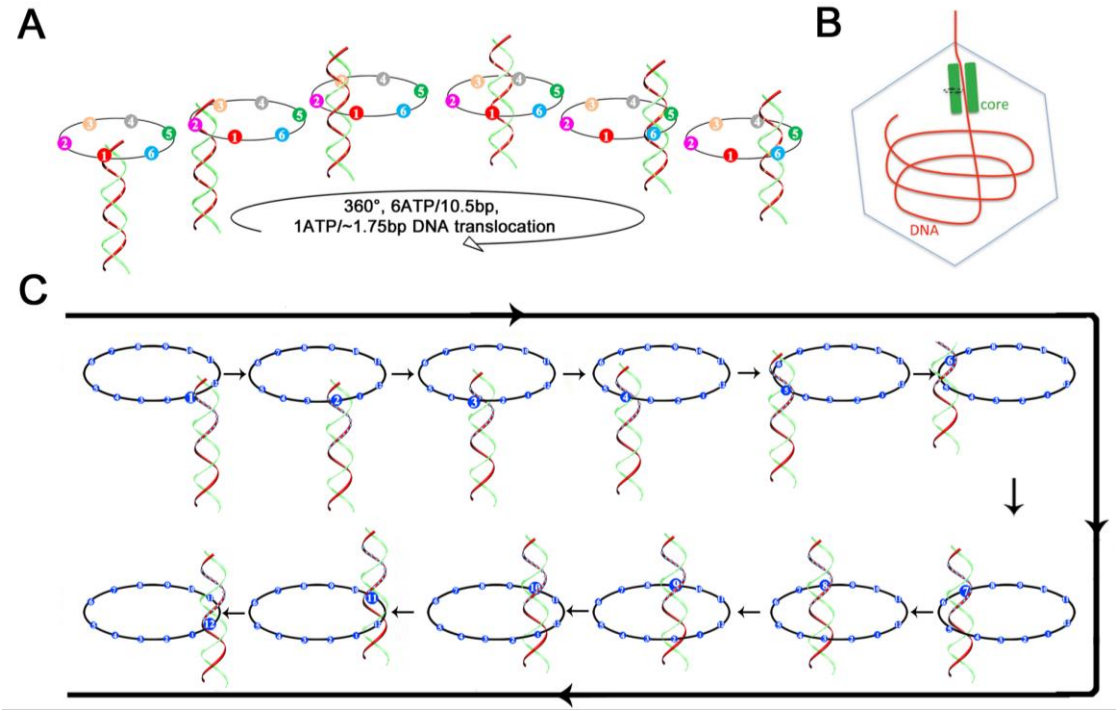

Fig. 8. Schematic showing the mechanism of sequential revolution in translocating dsDNA. A. The binding of ATP to one ATPase subunit stimulates the ATPase gp16 to adopt a conformation with a higher affinity for dsDNA. ATP hydrolysis forces gp16 to assume a new conformation with a lower affinity for dsDNA, thus pushing dsDNA away from the subunit and transferring it to an adjacent subunit. Rotation of neither the hexameric ring nor the dsDNA is required since the dsDNA revolves around the inner side of the ATPase ring. In each transitional step, one ATP is hydrolyzed, and in one cycle, six ATPs are required to translocate dsDNA one helical turn of 360° (10.5 bp). An animation is available at http://nanobio.uky.edu/movie.htm (adapted from Schwartz et al., 2013b with permission of the Elsevier). B. Diagram of CryoEM results showing offset of dsDNA in the channel of bacteriophage T7 DNA packaging motor. The dsDNA did not appear in the center of the channel, instead, the dsDNA tilted toward the wall of the motor channel (adapted from Guo et al., 2013awith the permission of the National Academy of Sciences). C. The revolution of dsDNA along the 12 subunits of the connector channel (adapted from Schwartz et al., 2013b with permission of the Elsevier).

they used their own logical and insightful view to piece together their findings independently (Kumar and Grubmuller, 2014 in press).

4. The dsDNA packaging motor of many, if not all, dsDNA bacteriophage uses the same revolution mechanism without rotation

All the dsDNA viruses known so far use a similar mechanism to translocate their genomic DNA into preformed protein shells, termed procapsids, during replication (For reviews, see (Guo and Lee,2007.; Rao and Feiss,2008.; Serwer,2010.; Zhang et al.,2012.)). It has been reported that the motors of bacteriophages phi29, HK97, SPP1, P22 and T7 share a common revolution mechanism without rotation (De-Donatis et al.,2014.). The special structure of these motors composes several factors that coordinate to drive the dsDNA with a one-way traffic mechanism. The 30° left-handed twist of the channel wall produces an anti-chiral arrangement with the right-handed helix of the dsDNA, resulting in a one-orientation trend. The same anti-chiral arrangement with the 30° left-handed twist has also been found in motor channels of other dsDNA viruses including phi29 (Guasch et al.,1998.), HK97 (Cardarelli et al.,2010.), SPP1 (Lhuillier et al.,2009.), P22 (Cingolani et al.,2002.) and T7 (Agirrezabala et al.,2005.). Of these motor channels, the primary amino acid sequences were not conserved, while the 2D (Agirrezabala et al., 2005) and 3D structures of the swivel are perfectly conserved and aligned (Fig. 11). Distinction of revolution from rotation by channel size and chirality is applicable to bacteriophages SPP1, HK97, P22, T4, T7 and phi29. Unidirectional flow loops within the channel of SPP1 and phi29 promote one-directional processing for the one-way trafficking of dsDNA (Fig. 12). The electropositive lysine layers present in all phage channels interact with a single strand of the electronegative dsDNA phosphate backbone (Fig. 5B, 5C), resulting in a relaying contact that facilitates one-way motion and generation of transitional pausing during dsDNA translocation. Coordination of these vector in the same direction makes viral DNA-packaging motors unusually effective.

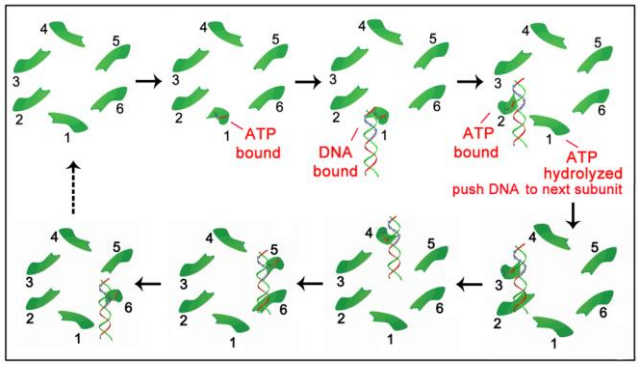

Fig. 9. Model of the mechanism of sequential action of phi29 DNA packaging motor. Binding of ATP to the conformationally disordered ATPase subunit stimulates an entropic and conformational change of the ATPase, thus fastening the ATPase at a less random configuration. This lower entropy conformation enables the ATPase subunit to bind dsDNA and prime ATP hydrolysis. ATP hydrolysis triggers the second entropic and conformational change,which renders the ATPase into a low affinity for dsDNA thus pushing the DNA to the next subunit that has already bound ATP. These sequential actions promote the movement and revolution of the dsDNA around the hexameric ATPase ring.

The revolution mechanism is in consent with the finding in many viruses revealing that their dsDNA is spooled inside the viral capsid, which occurs naturally and automatically, free from rotation tangles. The finding of hexamer formation for the DNA packaging machines is also in close agreement but might not be a coincidence with the structure of the ejection machine of dsDNA phages such as T7 (Fig. 10D) (Hu et al., 2013) and Epsilon 15 (Fig. 10C) (Jiang et al., 2006) used for host cell infection (Jiang et al., 2006; Lander et al., 2006; Molineux and Panja, 2013; Petrov and Harvey, 2008, , Tang et al., 2008; Duda and Conway, 2008; Cheng et al., 2013; Cerritelli et al., 1997; Cuervo et al., 2013; Panja and Molineux, 2010) (Fig. 10). A random arrangement occurs at first, with or without a free end, followed by a more ordered orientation of DNA as it continues to enter the procapsid. In phi29, the dsDNA has been found to show as a ring of density encircling around the gate region of the connector and to traverse the connector-tail tube (Fig. 10A) (Duda and Conway, 2008; Tang et al., 2008). The alternative explanation of the observation of such toroidal structure revealed by cryo-EM might be the consequence of the averaging effect of DNA revolution, since cryoEM is a collective image of many isolated dsDNA densities, the accumulation of the density of individual revolving intermediates with DNA tilted to the channel wall will produce a toroidal image. The force generation mechanism of viral DNA packaging motors has been investigated by using the members of the ASCE family, which have Walker A and Walker B motifs. These motifs convert energy from the binding or hydrolysis of ATP into a mechanical force, a process that usually involves a conformational change of ATPase (see next section). The spooling phenomenon caused by revolution is also evident in 382 some FtsK DNA pumps (Fig. 13) (Demarre et al., 2013; Grainge, 2013).

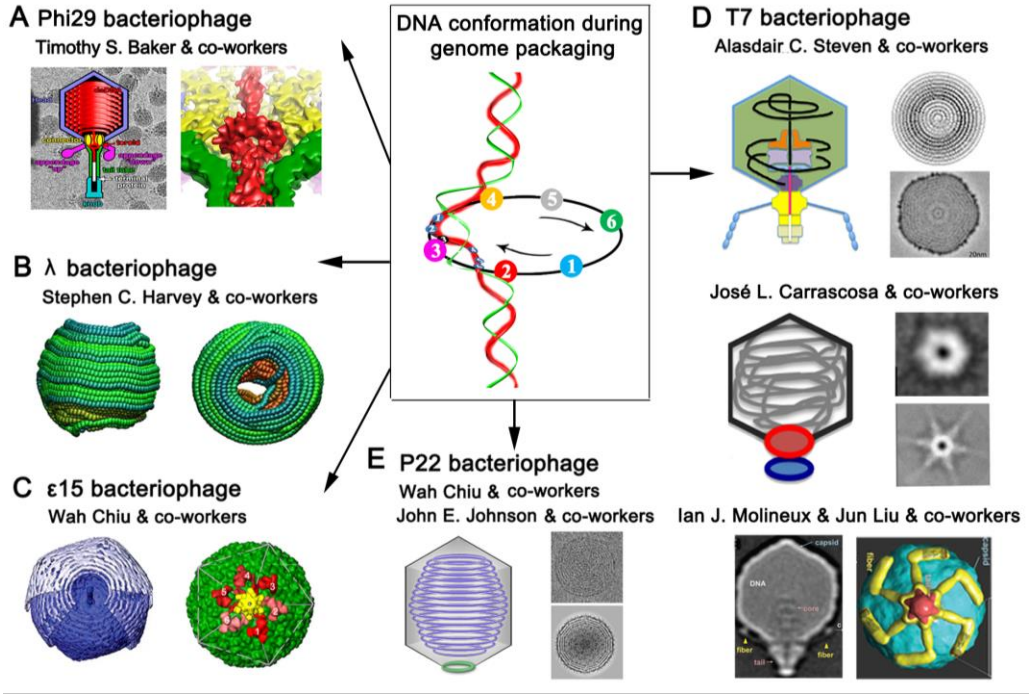

Fig. 10. Spooling of DNA within capsids of phages to support the revolution mechanism. The DNA spooling inside the capsids are shown using example of A. phi29 bacteriophage (adapted from Duda and Conway, 2008 with permission from Elsevier and Tang et al., 2008 with permission from Elsevier), B. λ bacteriophage (adapted from Petrov and Harvey, 2011 with permission from Elsevier), C. ε15 bacteriophage (adapted from Jiang et al., 2006with permission from Nature Publishing Group), D. T7 bacteriophage (adapted from Cerritelli et al., 1997 with permission from Elsevier, Cheng et al., 2014 with permission from Elsevier , Cuervo et al., 2013 with permission from The American Society for Biochemistry and Molecular Biology, and Hu et al., 2013 with permission from The American Association for the Advancement of Science). E. P22 bacteriophage (adapted and redrew from Lander et al., 2006 and adapted from Zhang et al., 2000 with permission from Elsevier). The spooling of the DNA inside the phage procapsids and the formation of the toroid in A might be results of the DNA revolution motion during the packaging as elucidated in the middle of the figure. The hexameric arrangement in C and D are parts of the dsDNA ejection machines.

5. Cellular dsDNA translocases also use the revolution mechanism without rotation

The cellular components that show the high-level similarity to the hexameric revolution motor come from two families of bacterial motor proteins: The FtsK family, an ASCE DNA motor protein group that transports DNA and separates intertwined chromosomes during cell division (Iyer et al.,2004.; Snider et al.,2008.; Snider and Houry,2008.); and the SpoIIIE family (Demarre et al.,2013.), which is responsible for transportation of DNA from a mother cell into the pre-spore during the cell division of *Bacillus subtilis* (Bath et al.,2000.; Grainge,2008.). The FtsK and SpoIIIE DNA transportation systems rely on the assembly of a hexameric machine. Although the precise action mode for FtsK and SpoIIIE motor is still elusive, available evidence strongly suggests that both motors use a revolution mechanism to translocate dsDNA without rotation (Fig. 8 and 13). The translocation of dsDNA with 1.6-1.75 base per hexamer subunit of FtsK (Crozat and Grainge,2010.; Massey et al.,2006.) perfectly agrees with the quantification in phi29 DNA packaging motor that each ATPase subunit uses one ATP to package 1.75 nucleotide (Guo et al.,1987c.; Guo et al.,2013b.; Schwartz et al.,2013b.; Schwartz et al.,2013a.; Zhao et al.,2013.). The model in which dsDNA touches the internal surface of the hexameric ring (Crozat and Grainge,2010.) is in agreement with the revolution mechanism that only one strand, but not both, of the dsDNA touches the internal wall of the motor channel and revolves without rotation (Schwartz et al.,2013b.; Zhao et al.,2013.). The proposed model of 60° per step (Crozat and Grainge,2010.) is in agreement with the finding of 30° per step within the dodecamer connector channel of all dsDNA bacteriophages (Fig. 11) and 60° per steps within the phi29 ATPase gp16 (Guo et al.,2013b.; Schwartz et al.,2013b.; Schwartz et al.,2013a.; Zhao et al.,2013.).

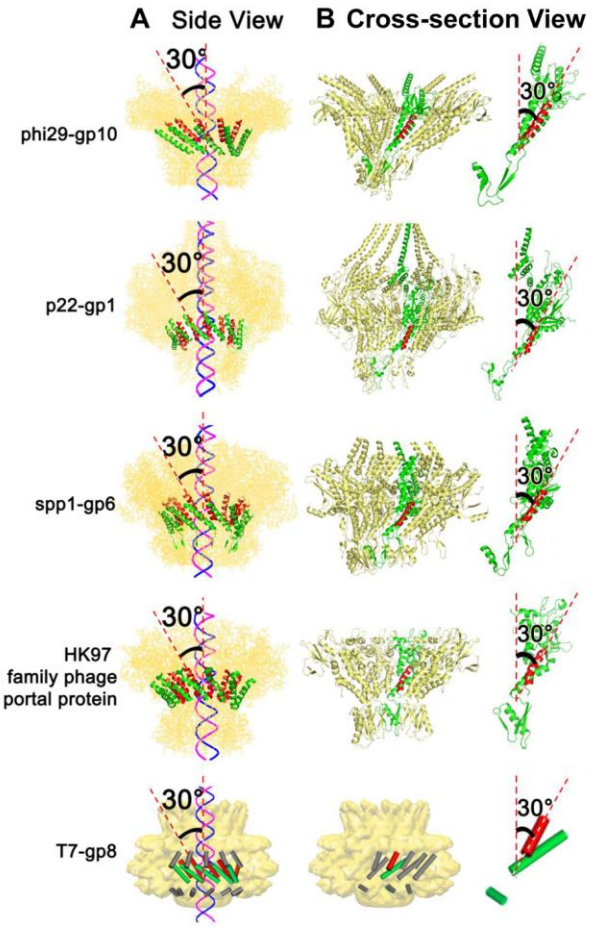

Fig. 11. Quaternary structures showing the presence of the left-handed 30° tilting of the connector channel of different bacteriophages. A and B column. The external view and the cross-section view, respectively, of the motor, showing the anti-chiral configuration between the left-handed connector subunits and the right-handed dsDNA helices. The 30° tilt of the helix (highlighted) relative to the vertical axis of the channel can be seen in a cross-section internal view of the connector channel and the view of its single subunit as shown in B (phi29 adapted from Schwartz et al., 2013b with permission from Elsevier, and adapted from De-Donatis et al., 2014 with permission from BioMed Central). T7 adapted from Agirrezabala et al., 2005 with permission from Elsevier. (PDB IDs: Phi29-gp10, 1H5W. (Guasch et al., 2002); HK97 family-portal protein, 3KDR; SPP1-gp6, 2JES. (Lebedev et al., 2007); P22-gp1, 3LJ5. (Olia et al., 2011), T7-gp8 EM ID: EMD-1231. (Agirrezabala et al., 2005)).

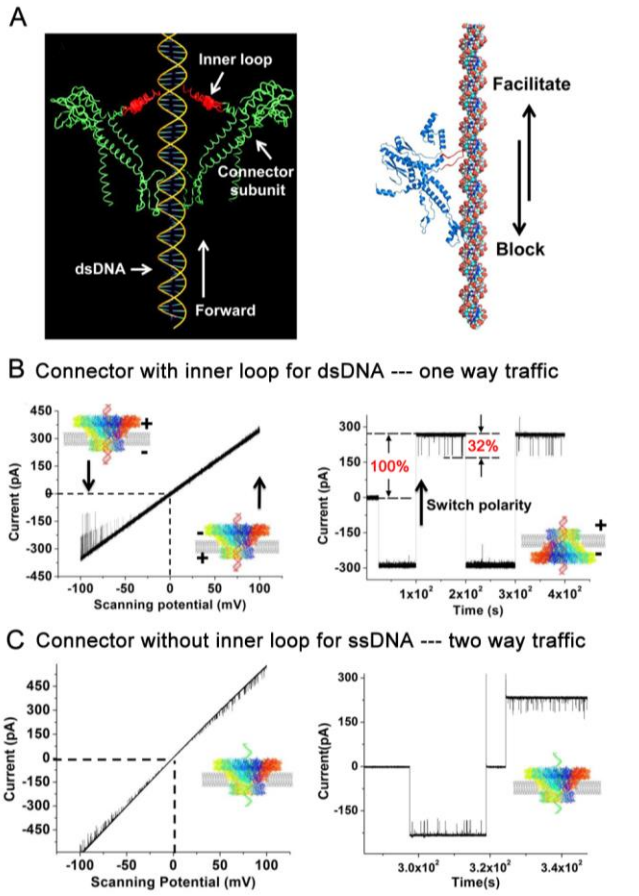

Fig. 12. The role of the flexible inner channel loop in DNA one-way traffic. A. Flexible loops within connector channels function as a valve to interact with DNA, facilitating DNA to move forward but blocking reversal of DNA during DNA packaging. B. Demonstration of one-way traffic of dsDNA through wild type connectors using a ramping potential and by switching polarity (right). C. SsDNA is translocated via two-way traffic with a loop deleted connector (adapted from Zhao et al., 2013 with permission from American Chemical Society).

5.1. FtsK

FtsK is responsible for dsDNA bidirectional translocation and conjugation between bacterial cells (Burton and Dubnau,2010.; Pease et al.,2005.). It is a multi-domain protein consisting of a 600-amino acid linker, a C-terminal ATPase domain FtsK(C) containing α, β and γ domains, and a N-terminal membrane-spanning domain FtsK(N) (Aussel et al.,2002.; Barre et al.,2000.; Yu et al.,1998.). The ability of FtsK to move on DNA molecules *in vitro* using ATP as the energy source suggests that it is a DNA motor protein (Pease et al.,2005.). The crystal structure of FtsK(C) indicates a ring-like hexamer (Lowe et al.,2008.; Massey et al.,2006.). Electron microscopy (EM) of FtsK(C) has revealed a DNA-dependent hexamer formation and DNA passage through the hexameric ring. Based on these data, a rotary inchworm mechanism has been proposed for FtsK to translocate dsDNA (Crozat and Grainge,2010.; Massey et al.,2006.) with ATPase subunits acting in a sequential manner (Fig. 13). Hexameric FtsK(C) translocates DNA through its central channel where protein-DNA contacts involve one or two hexamers. During each cycle of ATP binding and hydrolysis within each FtsK subunit, one motif binds tightly to the helix while the other progresses forward along the dsDNA. Such process that causes translational movement of the dsDNA is repeated by the subsequent handing off of the helix to the next adjacent subunit (Massey et al.,2006.). A monomer undergoes a catalytic cycle in which DNA translocates 1.6-1.75 bp with little rotation. Then DNA binds to the next subunit after the catalysis of a second subunit (Massey et al.,2006.). The hexameric ring holds dsDNA, with one functional subunit contacting the DNA at a time. The monomer of the functional subunit experiences an ATP catalytic cycle and translocates DNA through the channel by the hinged movement of the α domain and the β domain. This action carries the DNA backbone to the next functional subunit inside the same ring by a sequential hand-off mechanism. It performs the same exercise of DNA-binding, catalytic cycling and translocation. Such a cycle of DNA translocation is facilitated by the interaction between helical structure of DNA and the functional subunit of the hexameric ring without rotation of the protein ring against the DNA (Massey et al.,2006.). Furthermore, the cycle of DNA translocation may follow a sequential escort mechanism in which, at one catalytic step, multiple α and/or β domains interact with DNA, drag the strand, and release it until they change hands with the adjacent domains so that DNA is moved (Crozat et al.,2010.).

5.2. SpoIIIE

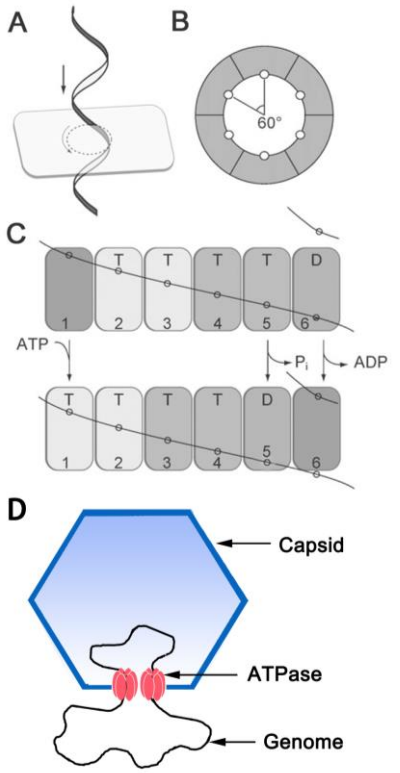

Fig. 13. Bacterial hexameric DNA translocase FtsK (A-C) and mimivirus (D) might also uses revolution mechanism. A. Diagram showing the contact of one strand of the dsDNA to the inner channel wall of the hexameric ATPase. The adjacent contact between DNA and ATPase will move around the inner surface of the channel without any rotation of the ATPase or DNA. B. Each of DNA contact points is expected to be separated by 60° along the inner surface of the ATPase hexameric channel. C. Sequential action of dsDNA translocation. DNA is shown as a line. T for ATP-bound and D for ADP-bound (adapted from Crozat and Grainge, 2010 with permission from John Wiley and Sons). D. Speculation for the segregation and translocation of the mimivirus genome into the capsid via revolution mechanism similar to FtsK (adapted from Chelikani et al., 2014).

Like FtsK, SpoIIIE shares a conserved C-terminal domain that harbors three subdomains, α, β, and γ (Fiche et al.,2013.; Kaimer and Graumann,2011.). The α and β subdomains translocate DNA through ATP binding and DNA-dependent hydrolysis (Barre,2007.), and the γ subdomain recognizes specific DNA sequences to guide DNA translocation (Lowe et al.,2008.; Sivanathan et al.,2006.). These subdomains assemble into a hexameric ring that accommodates dsDNA in its central channel (Massey et al.,2006.). The SpoIIIE DNA translocase actively moves DNA into the spore during *Bacillus subtilis* sporulation (Bath et al.,2000.; Sharp and Pogliano,2002.). The DNA translocation seems to be conducted by two hexamers, one within each membrane. One hexamer appears to pump DNA at a time, and then the other takes over. This view of DNA translocation receives support from the visualization of two chromosomal sites with both arms of the chromosome having moved simultaneously into the forespore. Further characterization of the SpoIIIE translocation pore assembly at the sporulation septum suggests a stepwise process (Fleming et al.,2010.). An unstable channel of DNA translocation is first formed by the transmembrane domain of SpoIIIE localized to the leading edge of the closing septum. This channel is stabilized by binding of DNA to the translocase domains, followed by DNA translocation through the separating membranes. The channel is destabilized with release of the DNA from the translocase domain. The destabilization generates a larger opening for the final loop of the circular chromosome to migrate into the forespore.

Recently, a conceptually alternative model for SpoIIIE/FtsK motors was proposed (Cattoni et al.,2013.). In contradiction with the previous model in which FtsK hexamer assembly is KOPS (FtsK Orienting/Polarizing Sequence) dependent (Graham et al.,2010.; Lowe et al.,2008.), it was shown that SRS (Sequence Retrieval System) sequences do not have a role in protein assembly by Fluorescence Correlation Spectroscopy and Atomic Force Microscopy. This new model involves three sequential steps: (a) binding of pre-formed hexamers to non-specific DNA, which might involve conformational transitions of the protein hexamer from an open- (inactive) to a closed-ring structure (active), (b) specific localization of SpoIIIE to SRS by target search exploration, and (c) sequence-specific activation of the motor mediated by binding and oligomerization of SpoIIIE-γ on SRS.

5.3 Large eukaryotic dsDNA viruses such as mimivirus and vaccinia virus

Recently, it has been reported that the motor components of the large eukaryotic dsDNA viruses, such as Acanthamoeba poylphaga mimivirus (APMV), display strong sequence similarity to FtsK and SPOIIIE motor components for the segregation and translocation, suggesting that the large dsDNA viruses might also use a revolution mechanism (Fig. 13D) (Chelikani et al., 2014). The large dsDNA viruses include mimivirus, vaccinia virus, pandoravirus. Whether vaccinia virus uses the same mechanism remains to be proved by further experimental data.

6. Rotational dsDNA translocases with only one ssDNA strand within the channel

Some hexameric dsDNA translocation motors such as RuvA/RuvB involved in DNA homologous recombination (Han et al.,2006.; Rafferty et al.,1996.) are sophisticated, and some other dsDNA riding motors such as those involved in DNA repair only display two protein subunits. The mechanisms of these motors are so complicated that they go beyond the scope of this review and will not be addressed here. Many of these ATPases are assembled into hexamers to rotate along nucleic acids with one strand of DNA or RNA passing through the channel. These rotation nanomotors include, but are not limited to, helicases (Bailey et al.,2007.; Castella et al.,2006.; Enemark and Joshua-Tor,2006.), DNA polymerase (Kato et al.,2001.), and RecA family proteins (Cox,2003.; Xing and Bell,2004b.), the latter of which plays a key role in genetic recombination and repair. Most rotation dsDNA translocases share the mechanisms that are distinct from the revolution dsDNA translocases.

6.1 Helicase DnaB

It has long been believed that the mechanism of translocation of single-stranded (ss) DNA or RNA operates by a rotation movement. A recent study from the crystal structure of the bacterial replicative DNA helicase DnaB has revealed that DnaB operates in the mechanism similar to the phi29 DNA packaging motor (Itsathitphaisarn et al.,2012.), but distinct from in the following respects: 1) the DNA inside the hexameric channel is a ssDNA instead of a dsDNA; 2) the motion is rotation instead of revolution; 3) the channel is right-handed instead of left-handed; and 4) the channel is small. DnaB is a hexameric motor that can unwind dsDNA in front of the replication fork to provide ssDNA templates for the DNA polymerase III holoenzyme (Kaplan and Steitz,1999.; LeBowitz and McMacken,1986.). Based on the crystal structure of the DnaB hexamer in a complex with GDP-AIF4 and ssDNA, a hand-over-hand translocation mechanism has been proposed by the Steitz group (Fig. 14). In this mechanism, the sequential hydrolysis of NTP is coupled to the 5′-3′ translocation of the subunits with a step size of two nucleotides, while some other helicases use the 3′-5′ direction (Thomsen and Berger,2009.). The sequential hand-by-hand migration of the individual subunits along the helical axis of an ssDNA template leads to DNA translocation (Fig. 14). Although the translocation substrate is ssDNA, it revolves as an A form structure;

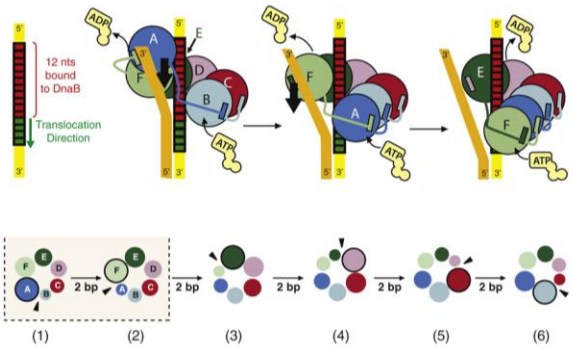

Fig. 14. Sequential rotation mechanism of the hexameric DNA helicase DnaB. One strand of the dsDNA displaces within the hexameric channel and the other strand is outside the ATPase channel (adapted from Itsathitphaisarn et al., 2012 with permission from Elsevier).

that is, the ssDNA is present in the complex as a helix similar to a dsDNA helix, albeit smaller in diameter, during translocation.

6.2 TrwB

TrwB structurally resembles ring helicases and F_1-ATPase because of its spherical nature and membrane (Gomis-Ruth et al.,2001.; Gomis-Ruth and Coll,2001.; Matilla et al.,2010.; Tato et al.,2007.). It is a homo-hexamer of the TraG-like family responsible for bacterial conjugation (Cabezon and de la,2006.). Its single hexamer is 110 Å in diameter and 90 Å in height with a channel ~20 Å wide. A ring of asparagine residues plugs the channel at the other end resulting in narrow end ~8 Å in diameter (Gomis-Ruth et al.,2001.). Crystallographic structural analysis has revealed that the cytoplasmic domain of TrwB is hexameric (Gomis-Ruth et al.,2001.). Its structural similarities to other well-documented DNA motors suggest that TrwB may translocate ssDNA through its central channel with energy derived from ATP hydrolysis. The central channel in TrwB could be occupied by a single DNA strand, which might be transferred through the internal cavity in a 5′-3′ direction (Cabezon and de la,2006.). This notion receives support from biochemical data showing that TrwB is a DNA-dependent ATPase (Tato et al.,2005.) and a structure-specific DNA-binding protein (Matilla et al.,2010.), likely to pump DNA by a "binding change mechanism" assigned to F_1-ATPase (Cabezon and de la,2006.). The ATPase activity is stimulated by interacting with TrwA (Tato et al.,2007.), a tetrameric *oriT*-specific DNA-binding protein (Moncalian and de la,2004.). Maximal ATPase rates can be reached in the presence of TrwA and dsDNA (Tato et al.,2007.). These findings lead to a model of DNA translocation that occurs toward the membrane through the TrwA-TrwB interaction.

6.3 RecA

The RecA family of ATP-dependent recombinases plays a crucial role in genetic recombination and dsDNA break repair in Archaea, Bacteria, and Eukaryota. Extensive biochemistry, genetics, electron microscopic X-ray crystallography studies have been carried out for the RecA family proteins (Dunderdale and West,1994.; Kowalczykowski and Eggleston,1994.). RecA can interacts with ssDNA to form right-handed filament with ssDNA as a complex, which is the only active form of the protein, with approximately six monomers of RecA per helical turn (Di et al.,1982.). The interaction can be enhanced by the binding of ATP (Menetski and Kowalczykowski,1985.). EM studies of the active filament has revealed that ATP binding triggers a re-orientation between the RecA ATPase domains, leading to the relative rotation of the protein on DNA substrate during the translocation of DNA by the energy of ATP hydrolysis.

7. Revolution and rotation mechanisms can be distinguished by motor channel size

If dsDNA advances through the center of the motor channel, the channel needs to have a size similar to the diameter of dsDNA. Thus, the diameter of the channel should be close to 2 nm for dsDNA or

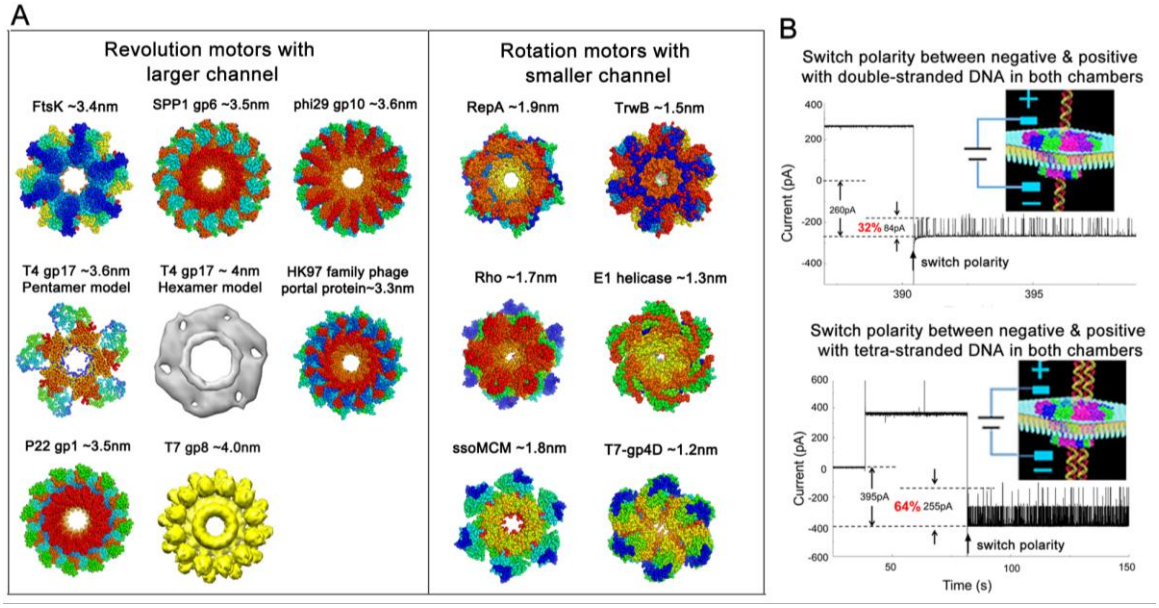

Fig. 15. Determination of the channel size of the DNA translocases. A. Comparison of the size of channels between biomotors using revolution mechanism(left panel) and biomotors using rotation mechanism (right panel). The dsDNA biomotors with a channel size of twice the width of dsDNA argues against the proposed bolt and nut treading mechanism, supporting the conclusion of revolution rather than rotation (adapted from Agirrezabala et al., 2005 with permission from Elsevier, adapted from Sun et al., 2008 with permission from Elsevier and adapted from De-Donatis et al., 2014 with permission from BioMed Central). (PDB IDs: RepA, 1G8Y. (Niedenzu et al., 2001); TrwB: 1E9R. (Gomis-Ruth et al., 2001); ssoMCM, 2VL6. (Liu et al., 2008); Rho, 3ICE. (Thomsen and Berger, 2009); E1, 2GXA. (Enemark and Joshua-Tor, 2006); T7-gp4D, 1E0J. (Singleton et al., 2000); FtsK, 2IUU. (Massey et al., 2006); Phi29-gp10, 1H5W. (Guasch et al., 2002); HK97 family-portal protein, 3KDR; SPP1-gp6, 2JES. (Lebedev et al., 2007); P22-gp1, 3LJ5. (Olia et al., 2011). T7-gp8 EMID: EMD-1231. (Agirrezabala et al., 2005)). B. Single-pore conductivity assay for the translocation of double- and tetra-stranded DNA through phi29 portal channel, revealing that the channel allowed one-way translocation of dsDNA with a blockade of ~31% (upper pannel) and tetra-stranded DNA with the blockade of ~64% (lower pannel), in agreement with the conclusion of the large size of the phi29 connector channel (adapted from De-Donatis et al., 2014 with permission from BioMed Central, and adapted from; Haque et al., 2014).

1nm for ssDNA so that DNA can touch the channel wall while passing through the channel. For revolution motors, however, dsDNA advances by touching the channel wall instead of proceeding through the center of the channel. Thus, the channel should be much larger than the diameter of the DNA so that there is sufficient room for revolution. By inspecting the crystal structures of different motors, the diameter of the channel of the revolution motor is larger than 3 nm and the rotation motor is smaller than 2 nm (De-Donatis et al.,2014.). The revolution of dsDNA along the hexametric ATPase ring is evidenced by the following parameters: the width of dsDNA helix is 2 nm, but the diameter of the narrowest region of the all connector channels of phi29, SPP1, T4, T7, HK97, and FtsK is 3-5 nm, as revealed by X-ray crystallography (Fig. 15) (Agirrezabala et al.,2005.; Lebedev et al.,2007.; Massey et al.,2006.; Sun et al.,2008.; Valpuesta and Carrascosa,1994; Simpson et al., 2000.). Here the 3-5 nm refers to the narrowest region of the channel and the other regions of the channel are much larger than 3-5 nm in diameter. Such a size ratio makes it impossible to exercise the bolt-and-nut-tracking mechanism, since for any instantaneous contact, the twisting of the DNA helix is required for rotation, however, with such a large channel, only one, but not two or more, ATPase subunit can touch the DNA (De-Donatis et al.,2014.). This channel size has been further proved by the single-pore conductivity assay carried out for the test of both dsDNA and tetra-stranded DNA translocation through the connector channel of the phi29 dsDNA packaging motor (Fig. 15B). The results demonstrated that phi29 translocated either dsDNA or tetra-stranded DNA, which occupied ~31% or ~64%, respectively, of the narrowest part of the channel (De-Donatis et al., 2014; Haque et al., 2014 submitted). The DNA packaging motor of phage T4 can package budged dsDNA with a 1, 2, 5, or up to 10-base internal mismatched structure, suggesting that the motor could allow DNA larger than 2 nm to pass the channel and supporting the finding that the channel of the revolution motor is larger than the diameter of the dsDNA (Oram et al., 2008).

During revolution of dsDNA through the channel, dsDNA advances by touching the channel wall instead of proceeding through the center of the channel (Guo et al.,2013a.). This is consistent with recent finding by Cryo-EM-imaging, showing that the T7 dsDNA core tilts from its central axis. A clear pattern indicates that the DNA core stack does tilt. A counterclockwise motion of the dsDNA was observed from the N-terminus when the connector was placed at the top (Guo et al.,2013a.) (Fig. 8B). This is in agreement with direction of clockwise revolution of dsDNA viewed from the wider end (C-terminus) to the narrower end (N-terminus) of the phi29 connector (Jing et al.,2010.; Schwartz et al.,2013b.; Zhang et al.,2012.; Zhao et al.,2013.) (Fig. 8).

8. Revolution motors can be distinguished from rotation motors by detecting channel chirality

A bolt-and-nut rotation mechanism requires that both treads of the bolt-and-nut display at the same orientation. However, the crystal structure of phi29 connector reveals an anti-chiral arrangement between motor connector subunit and the DNA helices (Fig. 11 and 16). All 12 subunits of the connector portal protein of phi29, tilt at a 30° left-handed angle relative to the vertical axis of the channel, form the channel in a configuration that runs anti-chiral to the right-hand dsDNA helix during packaging (Schwartz et al.,2013b.; Zhao et al.,2013.). This structural arrangement greatly facilitates the controlled motion, supporting the conclusion that dsDNA revolves, instead of rotates, through the connector channel touching each of the 12 connector subunits in 12 discrete steps of 30° transitions for each helical pitch, without producing a coiling or torsion force (Schwartz et al.,2013b.). Moreover, the 30° angle of each connector subunit coincides nicely with the crystal structure of the spiral cellular clamp loader and the grooves of dsDNA (Mayanagi et al.,2009.; McNally et al.,2010.). The conserved regions serve a common function in DNA packaging. They assemble into a propeller-like structure composed of 12 subunits with a central channel that acts as a pathway for the translocation of DNA. The 30° anti-chiral arrangement that plays a critical role in dsDNA packaging is conserved in evolution of the viral dsDNA motor proteins known so far.

The similarity in secondary structure pattern and quaternary structure of the portal proteins among phi29 and the other dsDNA tailed bacteriophages (SPP1, T7, T4, and HK97 family phages), particularly the 30° anti-chiral arrangement between the connector subunit and the DNA helices, provides strong evidence that the role the portal protein plays in phi29 DNA packaging is shared by all other dsDNA tailed bacteriophages (De-Donatis et al.,2014.). However, for rotation motors such as DnaB helicase (Itsathitphaisarn et al.,2012.), the channel displays right-handed twisting in contrast to the left-handed chirality found in the revolutionary viral DNA packaging motors (Schwartz et al.,2013b.; Zhao et al.,2013.) (Fig. 11 and 16).

9. Special aspects of motor actions

9.1. The viral DNA translocases transport dsDNA in one direction

The direction of translocation is controlled by five features in phi29 packing motor: 1) ATPase undergoes a series of entropy transitions and conformational changes during ATP and dsDNA binding. Hydrolysis of ATP results in a second change in conformation, possibly with an entropy alteration of the ATPase, one with a low affinity for dsDNA, causing it to push dsDNA to advance and revolve within the channel (Fig. 6 and 9). 2) The 30° angle of

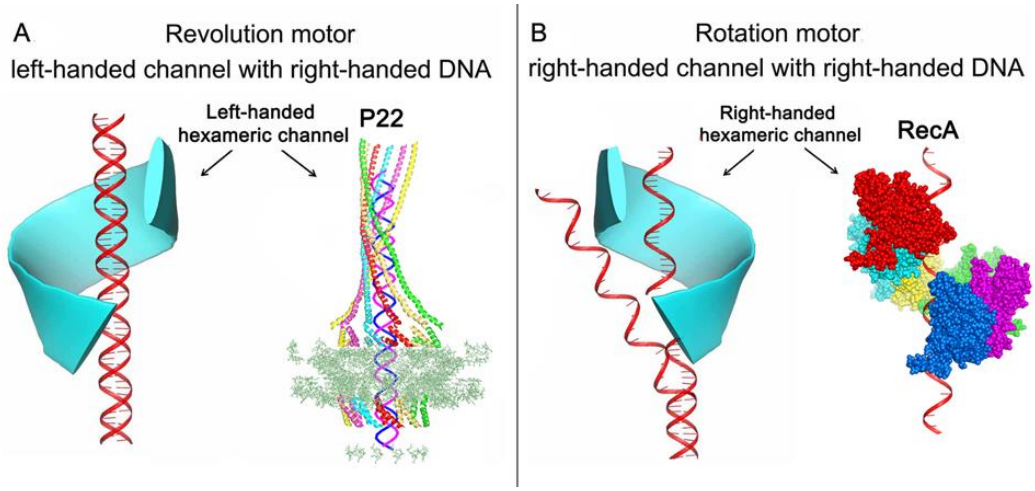

Fig. 16. The use of channel chirality to distinguish revolutionmotors fromrotation motors. A. In revolution motors, the right-handed DNA revolveswithin a left-handed channel (Guasch et al., 2002;Olia et al., 2011; Zhao et al., 2013). B. In rotationmotors, the right-handed DNA rotates through a right-handed channel via the parallel thread,with RecA (Xing and Bell, 2004a) and DnaB (Itsathitphaisarn et al., 2012) shown as examples (adapted from De-Donatis et al., 2014 with permission from BioMed Central). (PDB IDs: RecA, 1XMS. (Xing and Bell, 2004b); P22-gp1, 3LJ5. (Olia et al., 2011)).

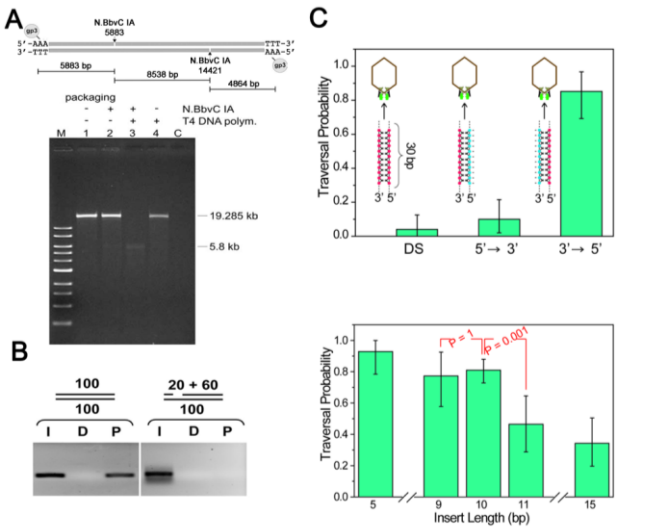

Fig. 17. Assay to demonstrate single strand unique directional revolution of dsDNA, and effect of DNA chemistry and structure on its packaging. A. Demonstration of blockage of dsDNA packaging by single-stranded gaps. When a single-stranded gap is present, only the left-end fragment of phi29 genomic DNA is packaged (adapted from Moll and Guo, 2005 with permission from Elsevier). B. T4 DNA packaging assays reveal that single stranded extensions with less than 12 bases at the DNA end do not inhibit translocation, whereas the ones with more bases do have a significant effect on the packaging (adapted from Oramet al., 2008with permission from Elsevier). C. Chemical modification of the negatively charged phosphate backbone on DNA packaging. Modification on the 3′→5′ strand does not block dsDNA packaging, but alternation on the other direction seriously affects DNA packaging (adapted from Aathavan et al., 2009 with permission from Nature Publishing Group). The results support the finding of the revolution mechanism showing that only one strand of the dsDNA interacts with the motor channel during revolution.

each subunit of the left-handed motor connector channel runs anti-chiral to the dsDNA helix, coinciding with the 12 subunits of the connector channel (360° ÷ 12 = 30°), as revealed by crystallography (Fig. 11 and 16). 3) The unidirectional flowing property of the internal channel loops serves as a ratchet valve to prevent dsDNA reversal. 4) The 5'-3' single-directional revolution of dsDNA advances with one strand contacting the phi29 motor connector channel wall (Fig. 5 and 8). 5) Four lysine layers interact with a single strand of the dsDNA phosphate backbone (Fig. 5) (De-Donatis et al.,2014.; Fang et al.,2012.; Jing et al.,2010.; Zhao et al.,2013.).

The one-way flow loops within the channel facilitate DNA moving towards the capsid but not reversing (Fig. 12). The dsDNA runs through the connector, potentially making sequential contact at each subunit. A mutant connector was constructed with the deletion of the internal loop containing residues 229-246. The mutant procapsids with the loop-deleted connector failed to produce any virion. The packaged dsDNA reversed its direction and slided out of the mutant procapsid after being packaged (Fang et al.,2012.; Geng et al.,2011.; Grimes et al.,2011.; Isidro et al.,2004.; Serwer,2010.). These results suggest that the channel loops act as a ratchet during DNA translocation to prevent the DNA from leaving, in line with the "push-through one-way valve" model (Fang et al.,2012.; Jing et al.,2010.; Zhang et al.,2012.; Zhao et al.,2013.). The connector is a one-way valve that only allows dsDNA to move into the procapsid unidirectionally, and the two-way traffic property has never been detected for wild type connectors under experimental conditions (Jing et al.,2010.). However, when all of the internal loops were deleted, translocation of dsDNA through the connector was blocked, as demonstrated by single pore conductance assay (Fang et al.,2012.), and the one-way traffic channel became two-way traffic for ssRNA or ssDNA (Geng et al.,2013.). The channel loops might act as a clamp; when internal loops of the connector were deleted, two-way traffic of DNA was observed, as demonstrated by both scanning potential and polarity switch (Geng et al.,2013.; Zhao et al.,2013.). Analysis of the crystal structure and Cryo-EM density map of SPP1 channel loops reveals that these loops are located in a close proximity to dsDNA *via* non-ionic interactions. The channel loops of phi29 and SPP1 might play similar roles in directional traffic of dsDNA to enter the capsid through the connector channel (Orlova et al.,2003.).

The 5'-3' single-directional movement along one strand advances DNA towards the capsid without reversal. The packaging direction is from 5' to 3', and dsDNA is processed by contacting the connector with one strand of DNA in the 5' to 3' direction, as modification of phi29 genome DNA in the 5' to 3' direction strand was found to stop dsDNA packaging (Aathavan et al.,2009.) (Fig. 17). It has also been demonstrated in Phi29 motor using gapped DNA (Fig. 17A). If the motor moves along the 5'-3' strand, it is expected that a 5.8kb DNA fragment will be packaged. On the other hand, if the motor moves along the 3'-5' strand, it is expected that a 14.3kb DNA fragment will be packaged. The empirical data showed that only the 5.8kb while not the 14.3kb DNA fragment was packaged, suggesting that the motor is moving along the DNA from 5' to 3' direction (Moll and Guo, 2005). One complete circle of revolution is equal to one helical turn of 10.5 base pairs of dsDNA. The dsDNA revolves along the motor using a single strand in the 5' to 3' direction (Oram et al.,2008.). It has been reported that a 3' single-strand overhang could be packaged under conditions extending from the 100 bp duplex. Extensions up to 12 bases at the end of the DNA did not inhibit the initiation of translocation. However, extensions to 20 or more bases significantly blocked the DNA packaging of the T4 motor (Fig. 17). The 20-base gap has been consistently found to be vulnerable, whether it was at the 3' end or in the middle of the DNA strand (Oram et al.,2008.). The finding of directional movement along only one strand of DNA answered the long term puzzle of contradictory reports (Abelson and Thomas, 1966; Hayward and Smith, 1972; Khan et al., 1995; Reddy and Gopinathan, 1986; Donohue et al., 1985; Kozloff et al., 1981; Kemper and Brown, 1976; Hsiao and Black, 1977; Zachary and Black, 1981; Zachary and Black, 1986; Pearson and Fox, 1988) on whether the single stranded gaps on DNA will block DNA packaging, since the result depends on which DNA strand displayed the gap. If the single stranded gap had the same length but displayed on different strands of 5' to 3' or 3' to 5', the answers of either block or unblock the DNA translocation are different.

9.2. Electrostatic interaction of lysine layers and phosphate backbone and mismatch between 10.5 bases per DNA patch and channel 12 subunits result in uneven steps in DNA translocation

The electrostatic force arises from the relay interaction of the electropositive lysine layers with the electronegative DNA phosphate backbone. The negatively charged phi29 connector interior channel surface is decorated with 48 positively charged lysine residues, as revealed by the connector crystal analysis (Guasch et al.,2002.) (Fig. 5). The residues that exist as four 12-lysine rings are derived from the 12 protein subunits that enclose the channel. DNA revolves through 12 subunits of the connector per cycle, with only one strand touching the channel wall. During a complete 360° revolution, the negatively charged phosphate backbone makes contact with the same positively charged layer of the lysine ring (Schwartz et al.,2013b.; Schwartz et al.,2013a.; Zhao et al.,2013.). This results in uneven speed with four pauses during the DNA translocation process (Chistol et al.,2012.; Schwartz et al.,2013b.; Zhao et al.,2013.).

The crystal structure shows that the length of the connector channel is 7 nm (Badasso et al.,2000.; Guasch et al.,2002.; Jimenez et al.,1986.) and four lysine layers fall vertically within a 3.7 nm range (Guasch et al.,2002.), spaced approximately ~0.9 nm apart on average. Since B-type dsDNA has a pitch of 0.34 nm/bp, ~2.6 bp exist for each rise along its axis that interact with the lysine ring (0.9

nm/0.34 nm·bp^{-1} = ~2.6 bp). For every 10.5 bp, one strand of DNA revolves 360° through the channel. This results in a 0.875 mismatch between the base with the negatively charged phosphate group and the channel subunits with positively charged lysine ring (10.5/12 = 0.875). Thus, four steps with each of 2.6 bp will be observed (0.875X(12/4)=2.6 bp). The dsDNA phosphate backbone interacts with the positively charged lysine in the next subunit, and the distance variation due to this mismatch is compensated for by the introduction of the next lysine layer. Thus, the contact point between the phosphate and the lysine shifts to a spot on the next lysine ring where the phosphate can make its next contact. This transition leads to a slight pause in DNA advancement. When dsDNA translocates through three subunits, the leading phosphate transitions into the next lysine layer in order to compensate for the imperfect match that occurs between the phosphate and each lysine residue during DNA advancement through the connector (Fig. 5). It has been found that the mutation of only one layer of the four lysine rings does not significantly affect motor action (Fang et al.,2012.), indicating that the interaction of lysine and phosphate is only an auxiliary force and not the main force involved in motor action. This also indicates that the uneven speed of the four steps of transition and pausing caused by the four lysine layers is not an essential function of the motor. The lysine layers and the 10.5 bases per helical turn are not a perfect match and the distance between layers is not constant. The lysine layers are also reported in the inner walls of the portal proteins of SPP1 and P22, which may potentially interact with their genomic DNA during packaging. Such pauses in speed during DNA translocation have been reported in both phi29 (Chistol et al.,2012.; Moffitt et al.,2009.) and T4 (Kottadiel et al.,2012.).

9.3. The motor transports concatemeric or closed circular dsDNA without breaking any covalent-bonds or changing topology of dsDNA

During cell segregation or binary fission, dsDNA translocases can transport circular dsDNA without breaking any covalent-bonds or changing topology of dsDNA (Bath et al.,2000.; Demarre et al.,2013.; Massey et al.,2006.). In most dsDNA viruses, the dsDNA substrate for packaging is the concatemer dsDNA (Bravo and Alonso,1990.; Everett,1981.; Jacob et al.,1979.; Son et al.,1988.; White and Richardson,1987.). How do the motors transport concatemers or closed circular dsDNA?

The ATPase monomer (not the hexamer) can bind to dsDNA (Schwartz et al.,2012.; Schwartz et al.,2013b.). After ATP binding, the ATPase subunit decreases in entropy and changes its conformation, leading to a high affinity for dsDNA thus assembling as a hexamer on DNA without requirement of ATP hydrolysis (De-Donatis et al.,2014.). Therefore, the motor assembles into a hexamer on the DNA itself, rather than the insertion or treading of the dsDNA molecule into a preformed hexameric ring. A free 5' or 3' dsDNA end is not required, and the motor can theoretically transport closed circular dsDNA without breaking covalent bonds or changing DNA topology.

It was commonly believed that the binding of ATPase gp16 to the viral procapsid to form a complex is the first step in motor function during DNA packaging (Fujisawa et al.,1991.; Guo et al.,1987b.). However, it has been found that the first step in phi29 DNA packaging is instead the binding of multiple gp16 in a queue along the dsDNA (Fig. 18A) (Schwartz et al.,2012.; Schwartz et al.,2013b.). A string of multiple Cy3-gp16 complexes have been observed on one dsDNA chain that has been lifted by, and stretched between, two polylysine-coated silica beads in the presence of non-hydrolysable ATPγS (Fig. 18A). This suggests that the queuing of ATPase gp16 along the DNA is the initial step in phi29 DNA packaging. Upon a conformational change stimulated by ATP binding, a single subunit gathers around the dsDNA chain first and then form a complex surrounding the DNA. It has been noted that both ends of the dsDNA are tethered to the beads, an observation which proves that a free 5' or 3' dsDNA end is not required for the ATPase to bind dsDNA, and that assembly of the hexameric gp16

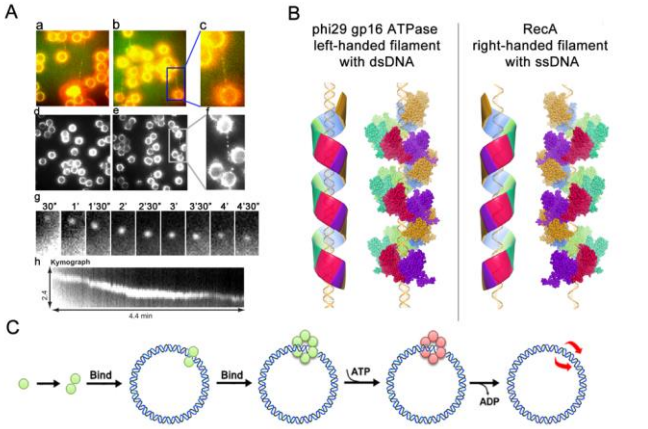

Fig. 18. Elucidation of how the motor transports closed circular or concatemeric dsDNA without breaking any covalent-bonds or changing the topology of the DNA. A. Direct observation of ATPase complexes queuing and moving along dsDNA. Cy3 conjugated gp16 were incubated with (a, b, e) and without (d) dsDNA tethered between two polylysine beads. The zoomed in images are shown in (c) and (f). The motion of the Cy3-gp16 spot was analyzed and a kymograph was produced to characterize the ATPase walking (g and h) (adapted from Schwartz et al., 2013b with permission from Elsevier). B. A model showing that gp16 hexamer acts as an open spiral filament similar to RecA filament with a different chirality rather than as a closed ring (adapted from De-Donatis et al., 2014 with permission from BioMed Central). C. Illustration of the assembly of the motor subunit on circular dsDNA. Subunits gather around the dsDNA chain first and then form a hexamer complex surrounding the DNA.

ring occurs only upon binding to DNA (Fig. 18). EM images also reveal multiple gp16 complexes binding to phi29 genome (Schwartz et al.,2013b.).

9.4. Sequential action of the six subunits of the ATPase

Sequential action of phi29 DNA packaging motor was originally reported by Chen and Guo (Chen and Guo,1997b.) and subsequently confirmed by Bustamante and coworkers (Moffitt et al.,2009.). Hill constant determination and binomial distribution of inhibition assay have led to the conclusion that ATPase subunits work sequentially and cooperatively (De-Donatis et al.,2014.; Schwartz et al.,2013b.). This action enables the motor to work continuously without interruption, despite some observable pauses. Cooperativity among motor subunits allows the motor to continue to move without interruption, as deduced from the observation of the binding of dsDNA to only one gp16 subunit at a time. ATPase activity has been analyzed by studying the effects of the introduced mutant subunits on the oligomerization of gp16 (Chen et al.,1997.; Trottier and Guo,1997.). Increasing the amounts of Walker B mutants added to the overall gp16 oligomer failed to provide any significant effect on the rate of hydrolysis when ATPase activity was measured in the absence of dsDNA. However, when saturating amounts of dsDNA were added to the reaction, a strong negative cooperative effect was produced with a profile that mostly overlapped with a predicted profile in which one single inactive subunit was able to inactivate the whole oligomer. A predicted case was calculated from the binomial distribution inhibition assay (Chen et al.,1997.; Trottier and Guo,1997.); these results suggest that in the presence of dsDNA, a rearrangement occurs within the subunits of gp16 that enables them to communicate with each other and to "sense" the nucleotide state of the reciprocal subunit.

Binding of ATP to the conformationally disordered ATPase subunit stimulates an conformational change, with possible entropy alteration (De-Donatis et al.,2014.), of the ATPase, thus fastening the ATPase at a less random configuration (Fig. 9). This lower conformation entropy enables the ATPase subunit to bind dsDNA and prime ATP hydrolysis. Based on the fact that the size of the motor channel is much larger than the width of the dsDNA, in any

instantaneous time, only one ATPase subunit can touch the DNA, and only the subunit that is bound to the dsDNA at any given time is permitted to hydrolyze ATP. ATP hydrolysis triggers the second entropic and conformational change, which renders the ATPase into a low affinity for dsDNA, thus pushing the DNA to the next subunit that has already bound to ATP with a high affinity for dsDNA. These sequential actions will promote the movement and revolution of the dsDNA around the internal hexameric ATPase ring.

Translocation occurs while the other subunits are in a type of "stalled" or "loaded" state. This represents an extremely high level of coordination in the function of the proteins with their DNA substrate, perhaps the most efficient process of coupling energy production *via* ATP hydrolysis and DNA translocation of all viral motors known so far. An effective mechanism of coordination is apparent between gp16 and dsDNA through the hydrolysis cycle as means for regulation. The cooperativity and sequential actions among hexameric ATPase subunits (Chen and Guo,1997b.; Moffitt et al.,2009.) promote revolution of dsDNA along the channel. The contact between the connector and the dsDNA chain is transferred from one point on the phosphate backbone to another, in line with previous reports (Moffitt et al.,2009.). Formation of both gp16/procapsid complex and gp16 queue on DNA have been observed (De-Donatis et al.,2014.; Guo et al.,1987b.; Koti et al.,2008.; Schwartz et al.,2013b.). The finding has led to our proposal (De-Donatis et al.,2014.) that gp16 hexamer is not an closed ring, but an open spiral ring forming a filament similar to the RecA protein with different chirality (Fig. 18B) (Di et al.,1982.).

10. Potential applications of the revolution motor

The discoveries discussed in this review offer a series of possible answers to the puzzles that may lead to inventions in the motion world. The riding system along one string of dsDNA provides a platform for cargo transportation at the nanoscale, and a tool for studying force generation mechanisms in a moving world. The revolution mechanism itself offers a prototype or a hint for the design of new motors involving forward motion via a tract, such as that used by roller coasters, trolley cars, or a launcher for flying objects such as a rocket to depart from a helical tract without rotation of the object. The transition of dsDNA along 12 channel subunits offers a series of recognition sites on the dsDNA backbone and provides additional spatial variables to discriminate nucleotides based on distance parameters for nucleotide sensing. Nature has evolved a clever machine that translocates DNA double helix to avoid difficulties associated with rotation, e.g. DNA supercoiling. A video of dsDNA translocation can be found at nanobio.uky.edu/file/motion.avi.

Acknowledgements

We would like to thank Alasdair Steven, Lindsay Black, Ian Molineux, Norman R. Watts, Wen Jiang, Paulo Tavares, Chad Schwartz, Gian Marco De-Donatis for constructive communications. The work was supported by NIH grants R01 EB003730, R01 EB012135, and U01 CA151648 to PG, who is a co-founder of Kylin Therapeutics, Inc. and Biomotor and RNA Nanotech Development Co., Ltd. The content is solely the responsibility of the authors and does not necessarily represent the official views of NIH. Funding to Peixuan Guo's Endowed Chair in Nanobiotechnology position is by the William Farish Endowment Fund.

References

Aathavan K, Politzer AT, Kaplan A, Moffitt JR, Chemla YR, Grimes S, Jardine PJ, Anderson DL, and Bustamante C. Substrate interactions and promiscuity in a viral DNA packaging motor. Nature 2009;461:669-73.

Abelson J, Thomas CA Jr. The anatomy of the T5 bacteriophage DNA molecule. J Mol Biol 1966;18:262-91.

Agirrezabala X, Martin-Benito J, Valle M, Gonzalez JM, Valencia A, Valpuesta JM, and Carrascosa JL. Structure of the connector of bacteriophage T7 at 8A resolution: structural homologies of a basic component of a DNA translocating machinery. J Mol Biol 2005;347:895-902.

Aker J, Hesselink R, Engel R, Karlova R, Borst JW, Visser AJWG and de Vries SC. *In vivo* hexamerization and characterization of the Arabidopsis AAA ATPase CDC48A complex using forster resonance energy transfer-fluorescence lifetime imaging microscopy and fluorescence correlation spectroscopy. Plant Physiology 2007;145:339-50.

Ammelburg M, Frickey T, and Lupas AN. Classification of AAA+ proteins. J Struct Biol 2006;156:2-11.

Aussel L, Barre FX, Aroyo M, Stasiak A, Stasiak AZ, and Sherratt D. FtsK is a DNA motor protein that activates chromosome dimer resolution by switching the catalytic state of the XerC and XerD recombinases. Cell 2002;108:195-205.

Badasso MO, Leiman PG, Tao Y, He Y, Ohlendorf DH, Rossmann MG, and Anderson D. Purification, crystallization and initial X-ray analysis of the head- tail connector of bacteriophage phi29. Acta Crystallogr D Biol Crystallogr 2000;56 (Pt 9):1187-90.

Bailey, S, Eliason, WK, and Steitz, TA. Structure of hexameric DnaB helicase and its complex with a domain of DnaG primase. Science 2007;318:459-63.

Barre FX. FtsK and SpoIIIE: the tale of the conserved tails. Mol Microbiol 2007;66:1051-5.

Barre FX, Aroyo M, Colloms SD, Helfrich A, Cornet F, and Sherratt DJ. FtsK functions in the processing of a Holliday junction intermediate during bacterial chromosome segregation. Genes Dev 2000;14:2976-88.

Bath J, Wu LJ, Errington J, and Wang JC. Role of Bacillus subtilis SpoIIIE in DNA transport across the mother cell-prespore division septum. Science 2000;290:995-7.

Baumann RG, Mullaney J, and Black LW. Portal fusion protein constraints on function in DNA packaging of bacteriophage T4. Mol Microbiol 2006;61:16-32.

Bazinet C and King J. The DNA translocation vertex of dsDNA bacteriophages. Ann Rev Microbiol 1985;39:109-29.

Bravo A and Alonso JC. The generation of concatemeric plasmid DNA in Bacillus subtilis as a consequence of bacteriophage SPP1 infection. Nucleic Acids Res 1990;18:4651-7.

Burton B and Dubnau D. Membrane-associated DNA transport machines. Cold Spring Harb Perspect Biol 2010;2:a000406.

Cabezon E and de la CF. TrwB: an F(1)-ATPase-like molecular motor involved in DNA transport during bacterial conjugation. Res Microbiol 2006;157:299-305.

Cardarelli L, Lam R, Tuite A, Baker LA, Sadowski PD, Radford DR, Rubinstein JL, Battaile KP, Chirgadze N, Maxwell KL, and Davidson AR. The crystal structure of bacteriophage HK97 gp6: defining a large family of head-tail connector proteins. J Mol Biol 2010;395:754-68.

Carrascosa JL, Vinuela E, Garcia N, and Santisteban A. Structure of the head-tail connector of bacteriophage phi 29. J Mol Biol 1982;154:311-24.

Casjens SR. The DNA-packaging nanomotor of tailed bacteriophages. Nat Rev Microbiol 2011;9:647-57.

Caspar DLD and Klug A. Physical principles in the construction of regular viruses. Cold Spr Harb Symp Quant Biol 1962;27:1-24.

Castella S, Burgin D, and Sanders CM. Role of ATP hydrolysis in the DNA translocase activity of the bovine papillomavirus (BPV-1) E1 helicase. Nucleic Acids Res 2006;34:3731-41.

Cattoni DI, Chara O, Godefroy C, Margeat E, Trigueros S, Milhiet PE, and Nollmann M. SpoIIIE mechanism of directional translocation involves target search coupled to sequence-dependent motor stimulation. EMBO Rep 2013;14:473-9.

Cerritelli ME, Cheng N, Rosenberg AH, McPherson CE, Booy FP, and Steven AC. Encapsidated Conformation of Bacteriophage T7 DNA. Cell 1997;91:271-280.

Chang C, Zhang H, Shu D, Guo P, and Savran C. Bright-field analysis of phi29 DNA packaging motor using a magnetomechanical system. Appl Phys Lett 2008;93:153902-3.

Chelikani V, Ranjan T, Zade A, Shukla A, Kondabagil K. Genome segregation and packaging machinery in acanthamoeba polyphaga mimivirus is reminiscent of bacterial apparatus. J Virol. 2014;88:6069-75.

Chemla YR, Aathavan K, Michaelis J, Grimes S, Jardine PJ, Anderson DL, and Bustamante C. Mechanism of force generation of a viral DNA packaging motor. Cell 2005;122:683-92.

Chen C and Guo P. Magnesium-induced conformational change of packaging RNA for procapsid recognition and binding during phage phi29 DNA encapsidation. J Virol 1997a;71:495-500.

Chen C and Guo P. Sequential action of six virus-encoded DNA-packaging RNAs during phage phi29 genomic DNA translocation. J Virol 1997b;71:3864-71.

Chen C, Trottier M, and Guo P. New approaches to stoichiometry determination and mechanism investigation on RNA involved in intermediate reactions. Nucleic Acids Symposium Series 1997;36:190-3.

Chen YJ, Yu X, and Egelman EH. The hexameric ring structure of the Escherichia coli RuvB branch migration protein. J Mol Biol 2002;319:587-91.

Cheng N, Wu W, Watts NR, Steven AC. Exploiting radiation damage to map proteins in nucleoprotein complexes: The internal structure of bacteriophage T7. J Struct Biol 2014;185:250-6.

Chistol G, Liu S, Hetherington CL, Moffitt JR, Grimes S, Jardine PJ, and Bustamante C. High Degree of Coordination and Division of Labor among Subunits in a Homomeric Ring ATPase. Cell 2012;151:1017-28.

Cingolani G, Moore SD, Prevelige J, and Johnson JE. Preliminary crystallographic analysis of the bacteriophage P22 portal protein. J Struct Biol 2002;139:46-54.

Cox MM. The bacterial RecA protein as a motor protein. Ann Rev Microbiol 2003;57:551-577.

Crozat E and Grainge I. FtsK DNA translocase: the fast motor that knows where it's going. Chembiochem 2010;11:2232-43.

Crozat E, Meglio A, Allemand JF, Chivers CE, Howarth M, Venien-Bryan C, Grainge I, and Sherratt DJ. Separating speed and ability to displace roadblocks during DNA translocation by FtsK. EMBO J 2010;29:1423-33.

Cuervo A, Pulido-Cid M, Chagoyen M, Arranz R, González-García VA, Garcia-Doval C, et al. Structural characterization of the bacteriophage T7 tail machinery. J Biol Chem 2013;288:26290-9.

De-Donatis G, Zhao Z, Wang S, Huang PL, Fang H, Schwartz C, Tsodikov VO, Zhang H, Haque F and Guo P. Finding of widespread viral and bacterial 3 revolution dsDNA translocation motors distinct from rotation motors by channel chirality and size. Cell Biosci 2014 in press.

Demarre G, Galli E, and Barre FX. The FtsK Family of DNA Pumps. Adv Exp Med Biol 2013;767:245-62.

Di CE, Engel A Stasiak A, and Koller T. Characterization of complexes between recA protein and duplex DNA by electron microscopy. J Mol Biol 1982;157:87-103.

Dixit AB, Ray K, and Black LW. Compression of the DNA substrate by a viral packaging motor is supported by removal of intercalating dye during translocation. Proc Natl Acad Sci U S A 2012;109:20419-24.

Doan DN and Dokland T. The gpQ portal protein of bacteriophage P2 forms dodecameric connectors in crystals. J Struct Biol 2007;157:432-6.

Donohue TJ, Chory J, Goldsand TE, Lynn SP, Kaplan S. Structure and physical map of Rhodopseudomonas sphaeroides bacteriophage RS1 DNA. J Virol 1985; 55:147-57.

Duda RL and Conway JF. Asymmetric EM reveals new twists in phage phi29 biology. Structure 2008;16:831-2.

Dunderdale HJ and West SC. Recombination genes and proteins. Curr Opin Genet Dev 1994;4:221-8.
Enemark EJ and Joshua-Tor L. Mechanism of DNA translocation in a replicative hexameric helicase. Nature 2006;442:270-5.
Everett RD. DNA replication of bacteriophage T5. 3. Studies on the structure of concatemeric T5 DNA. J gen virol 1981;52:25-38.
Fang H, Jing P, Haque F, and Guo P. Role of channel Lysines and "Push Through a One-way Valve" Mechanism of Viral DNA packaging Motor. Biophysical Journal 2012;102:127-35.
Fiche JB, Cattoni DI, Diekmann N, Langerak JM, Clerte C, Royer CA, Margeat E, Doan T, and Nollmann M. Recruitment, assembly, and molecular architecture of the SpoIIIE DNA pump revealed by superresolution microscopy. PLoS Biol 2013;11:e1001557.
Fleming TC, Shin JY, Lee SH, Becker E, Huang KC, Bustamante C, and Pogliano K. Dynamic SpoIIIE assembly mediates septal membrane fission during Bacillus subtilis sporulation. Genes Dev 2010;24:1160-72.
Fujisawa H, Shibata H, and Kato H. Analysis of interactions among factors involved in the bacteriophage T3 DNA packaging reaction in a defined *in vitro* system. Virology 1991;185:788-94.
Geng J, Wang S, Fang H, and Guo P. Channel size conversion of Phi29 DNA-packaging nanomotor for discrimination of single- and double-stranded nucleic acids. ACS Nano 2013;7:3315-23.
Geng J, Fang H, Haque F, Zhang L, and Guo P. Three reversible and controllable discrete steps of channel gating of a viral DNA packaging motor. Biomaterials 2011;32:8234-42.
Gomis-Ruth FX and Coll M. Structure of TrwB, a gatekeeper in bacterial conjugation. Int J Biochem Cell Biol 2001;33:839-43.
Gomis-Ruth FX, Moncalian G, Perez-Luque R, Gonzalez A, Cabezon E, de la CF, and Coll M. The bacterial conjugation protein TrwB resembles ring helicases and F1-ATPase. Nature 2001;409:637-41.
Graham JE, Sherratt DJ, and Szczelkun MD. Sequence-specific assembly of FtsK hexamers establishes directional translocation on DNA. Proc Natl Acad Sci U S A 2010;107:20263-8.
Grainge I. Sporulation: SpoIIIE is the key to cell differentiation. Curr Biol 2008;18:R871-2.
Grainge I. Simple topology: FtsK-directed recombination at the dif site. Biochem Soc Trans 2013;41:595-600.
Grigoriev DN, Moll W, Hall J, and Guo P. Bionanomotor. In: Nalwa HS, editor. Encyclopedia of nanoscience and nanotechnology. American Scientific Publishers; 2004. p. 361-74.
Grimes S and Anderson D. The bacteriophage phi29 packaging proteins supercoil the DNA ends. J Mol Biol 1997;266:901-14.
Grimes S and Anderson D. RNA Dependence of the Bateriophage phi29 DNA Packaging ATPase. J Mol Biol 1990;215:559-66.
Grimes S, Ma S, Gao J, Atz R, and Jardine PJ. Role of phi29 connector channel loops in late-stage DNA packaging. J Mol Biol 2011;410:50-9.
Guasch A, Pous J, Ibarra B, Gomis-Ruth FX, Valpuesta JM, Sousa N, Carrascosa JL, and Coll M. Detailed architecture of a DNA translocating machine: the high-resolution structure of the bacteriophage phi29 connector particle. J Mol Biol 2002;315:663-76.
Guasch A, Pous J, Parraga A, Valpuesta JM, Carrascosa JL, and Coll M. Crystallographic analysis reveals the 12-fold symmetry of the bacteriophage phi29 connector particle. J Mol Biol 1998;281:219-25.
Guenther B, Onrust R, Sali A, O'Donnell M, and Kuriyan J. Crystal structure of the delta' subunit of the clamp-loader complex of E. coli DNA polymerase III. Cell 1997;91:335-45.
Guo F, Liu Z, Vago F, Ren Y, Wu W, Wright ET, Serwer P, and Jiang W. Visualization of uncorrelated, tandem symmetry mismatches in the internal genome packaging apparatus of bacteriophage T7. Proc Natl Acad Sci U S A 2013a;110:6811-6.
Guo P. Biophysical studies reveal new evidence for one-way revolution mechanism of biomotors (Editorial Comments: New and Notable). Biophys J 2014;106:1837-1838.
Guo P, Erickson S, and Anderson D. A small viral RNA is required for *in vitro* packaging of bacteriophage phi29 DNA. Science 1987a;236:690-4.
Guo P, Grimes S, and Anderson D. A defined system for *in vitro* packaging of DNA-gp3 of the *Bacillus subtilis* bacteriophage phi29. Proc Natl Acad Sci USA 1986;83:3505-9.
Guo P, Peterson C, and Anderson D. Initiation events in *in vitro* packaging of bacteriophage phi29 DNA-gp3. J Mol Biol 1987b;197:219-28.
Guo P, Peterson C, and Anderson D. Prohead and DNA-gp3-dependent ATPase activity of the DNA packaging protein gp16 of bacteriophage phi29. J Mol Biol 1987c;197:229-36.
Guo P, Schwartz C, Haak J, and Zhao Z. Discovery of a new motion mechanism of biomotors similar to the earth revolving around the sun without rotation. Virology 2013b;446:133-43.
Guo P, Zhang C, Chen C, Trottier M, and Garver K. Inter-RNA interaction of phage phi29 pRNA to form a hexameric complex for viral DNA transportation. Mol Cell 1998;2:149-55.
Guo P and Lee TJ. Viral nanomotors for packaging of dsDNA and dsRNA. Mol Microbiol 2007;64:886-903.
Han YW, Tani T, Hayashi M, Hishida T, Iwasaki H, Shinagawa H, and Harada Y. Direct observation of DNA rotation during branch migration of Holliday junction DNA by Escherichia coli RuvA-RuvB protein complex. Proc Natl Acad Sci U S A 2006;103:11544-8.
Haque F, Wang S, Stites C, Chen L, Wang C, Guo P. Single pore translocation of folded, double-stranded, and tetra-stranded DNA through channel of bacteriophage phi29 DNA packaging motor. 2014 [Submitted for publication].
Hayward G S, Smith MG. The chromosome of bacteriophage T5. I. Analysis of the single-stranded DNA fragments by agarose gel electrophoresis. J Mol Biol 1972;63:383-95.
Hendrix RW. Symmetry mismatch and DNA packaging in large bacteriophages. Proc Natl Acad Sci USA 1978;75:4779-83.
Hendrix RW. Bacteriophage DNA packaging: RNA gears in a DNA transport machine (Minireview). Cell 1998;94:147-50.
Hu B, Margolin W, Molineux IJ, Liu J. The bacteriophage T7 virion undergoes extensive structural remodeling during infection. Science 2013;339:576-9.
Hugel T, Michaelis J, Hetherington CL, Jardine PJ, Grimes S, Walter JM, Faik W, Anderson DL, and Bustamante C. Experimental test of connector rotation during DNA packaging into bacteriophage phi29 capsids. Plos Biology 2007;5:558-67.
Hsiao CL, Black LW. DNA packaging and the pathway of bacteriophage T4 head assembly. Proc Natl Acad Sci USA 1977; 74:3652-6.
Hwang Y, Catalano CE, and Feiss M. Kinetic and mutational dissection of the two ATPase activities of terminase, the DNA packaging enzyme of bacteriophage lambda. Biochemistry 1996;35:2796-803.
Ibarra B, Caston J.R., Llorca O., Valle M, Valpuesta J.M., and Carrascosa J.L. Topology of the components of the DNA packaging machinery in the phage phi29 prohead. J Mol Biol 2000;298:807-15.
Ibarra B, Valpuesta JM, and Carrascosa JL. Purification and functional characterization of p16, the ATPase of the bacteriophage phi29 packaging machinary. Nucleic Acids Res 2001;29:4264-73.
Isidro A, Henriques AO, and Tavares P. The portal protein plays essential roles at different steps of the SPP1 DNA packaging process. Virology 2004;322:253-63.
Itsathitphaisarn O, Wing RA, Eliason WK, Wang J, and Steitz TA. The hexameric helicase DnaB adopts a nonplanar conformation during translocation. Cell 2012;151:267-77.
Iyer LM, Makarova KS, Koonin EV, and Aravind L. Comparative genomics of the FtsK-HerA superfamily of pumping ATPases: implications for the origins of chromosome segregation, cell division and viral capsid packaging. Nucleic Acids Res 2004;32:5260-79.
Jacob RJ, Morse LS, and Roizman B. Anatomy of herpes simplex virus DNA: XII. Accumulation of head-to-tail concatemers in nuclei of infected cells and their role in the generation of the four isomeric arrangements of viral DNA. J Virol 1979;29:448-57.
Jiang W, Chang J, Jakana J, Weigele P, King J, and Chiu W. Structure of epsilon15 bacteriophage reveals genome organization and DNA packaging/injection apparatus. Nature 2006;439:612-6.
Jimenez J, Santisteban A, Carazo JM, and Carrascosa JL. Computer graphic display method for visualizing three-dimensional biological structures. Science 1986;232:1113-5.
Jing P, Haque F, Shu D, Montemagno C, and Guo P. One-Way Traffic of a Viral Motor Channel for Double-Stranded DNA Translocation. Nano Lett 2010;10:3620-7.
Kaimer C and Graumann PL. Players between the worlds: multifunctional DNA translocases. Curr Opin Microbiol 2011;14:719-25.
Kaplan DL and Steitz TA. DnaB from Thermus aquaticus unwinds forked duplex DNA with an asymmetric tail length dependence. J Biol Chem 1999;274:6889-97.
Kato M, Frick DN, Lee J, Tabor S, Richardson CC, and Ellenberger T. A complex of the bacteriophage T7 primase-helicase and DNA polymerase directs primer utilization. J Biol Chem 2001;276:21809-20.
Kemper B, Brown DT. Function of gene 49 of bacteriophage T4. II. Analysis of intracellular development and the structure of very fast-sedimenting DNA. J Virol 1976;18:1000-15.
Khan SA, Hayes SJ, Wright, ET, Watson RH, Serwer P. Specific single-stranded breaks in mature bacteriophage T7 DNA. Virology 1995;211:329 -31.
Kochan J, Carrascosa JL, and Murialdo H. Bacteriophage Lambda Preconnectors: Purification and Structure. J Mol Biol 1984;174:433-47.
Koti JS, Morais MC, Rajagopal R, Owen BA, McMurray CT, and Anderson D. DNA packaging motor assembly intermediate of bacteriophage phi29. J Mol Biol 2008;381:1114-32.
Kottadiel VI, Rao VB, and Chemla YR. The dynamic pause-unpackaging state, an off-translocation recovery state of a DNA packaging motor from bacteriophage T4. Proc Natl Acad Sci U S A 2012;109:20000-5.
Kowalczykowski SC and Eggleston AK. Homologous pairing and DNA strand-exchange proteins. Annu Rev Biochem 1994;63:991-1043.
Kozloff LM, Chapman V, DeLong S. Defective packing of an unusual DNA in a virulent Erwinia phage, Erh 1. Prog Clin Biol Res 1981;64:253-69.
Kumar R, Grubmuller H. Elastic properties and heterogeneous stiffness of the Phi29 motor 1112 connector channel. Biophys J 2014 ; 106:1338-48.
Lander GC, Tang L, Casjens SR, Gilcrease EB, Prevelige P, Poliakov A, Potter CS, Carragher B, and Johnson JE. The structure of an infectious P22 virion shows the signal for headful DNA packaging. Science 2006;312:1791-5.
Lebedev AA, Krause MH, Isidro AL, Vagin AA, Orlova EV, Turner J, Dodson EJ, Tavares P, and Antson AA. Structural framework for DNA translocation *via* the viral portal protein. EMBO J 2007;26:1984-94.
LeBowitz JH and McMacken R. The *Escherichia coli* dnaB replication protein is a DNA helicase. The Journal of Biological Chemistry 1986;261:4738-48.
Lee TJ and Guo P. Interaction of gp16 with pRNA and DNA for genome packaging by the motor of bacterial virus phi29. J Mol Biol 2006;356:589-99.
Lee TJ, Schwartz C, and Guo P. Construction of Bacteriophage Phi29 DNA Packaging Motor and its Applications in Nanotechnology and Therapy. Ann Biomed Eng 2009;37:2064-081.
Lee TJ, Zhang H, Liang D, and Guo P. Strand and nucleotide-dependent ATPase activity of gp16 of bacterial virus phi29 DNA packaging motor. Virology 2008;380:69-74.
Lhuillier S, Gallopin M, Gilquin B, Brasiles S, Lancelot N, Letellier G, Gilles M, Dethan G, Orlova EV, Couprie J, Tavares P, and Zinn-Justin S. Structure of bacteriophage SPP1 head-to-tail connection reveals mechanism for viral DNA gating. Proc Natl Acad Sci U S A 2009;106:8507-12.
Liu W, Pucci B, Rossi M, Pisani FM, and Ladenstein R. Structural analysis of the Sulfolobus solfataricus MCM protein N-terminal domain. Nucleic Acids Res 2008;36:3235-43.
Liu W, Pucci B, Rossi M, Pisani FM, Ladenstein R. Structural analysis of the Sulfolobus solfataricus MCM protein N-terminal domain. Nucleic Acids Res 2008; 36:3235-43.
Lowe J, Ellonen A, Allen MD, Atkinson C, Sherratt DJ, and Grainge I. Molecular mechanism of sequence-directed DNA loading and translocation by FtsK. Mol Cell 2008;31:498-509.
Maluf NK and Feiss M. Virus DNA translocation: progress towards a first ascent of mount pretty difficult. Mol Microbiol 2006;61:1-4.
Martin A, Baker TA, and Sauer RT. Rebuilt AAA+ motors reveal operating principles for ATP-fuelled machines. Nature 2005;437:1115-20.
Massey TH, Mercogliano CP, Yates J, Sherratt DJ, and Lowe J. Double-stranded DNA translocation: structure and mechanism of hexameric FtsK. Mol Cell 2006;23:457-69.
Matilla I, Alfonso C, Rivas G, Bolt EL, de la CF, and Cabezon E. The conjugative DNA translocase TrwB is a structure-specific DNA-binding protein. J Biol Chem 2010;285:17537-44.
Mayanagi K, Kiyonari S, Saito M, Shirai T, Ishino Y, and Morikawa K. Mechanism of replication machinery assembly as revealed by the DNA ligase-PCNA-DNA complex architecture. Proc Natl Acad Sci U S A 2009;106:4647-52.
McNally R, Bowman GD, Goedken ER, O'Donnell M, and Kuriyan J. Analysis of the role of PCNA-DNA contacts during clamp loading. BMC Struct Biol 2010;10:3.
Menetski JP and Kowalczykowski SC. Interaction of recA protein with single-stranded DNA. Quantitative aspects of binding affinity modulation by nucleotide cofactors. J Mol Biol 1985;181:281-95.
Moffitt JR, Chemla YR, Aathavan K, Grimes S, Jardine PJ, Anderson DL, and Bustamante C. Intersubunit coordination in a homomeric ring ATPase. Nature 2009;457:446-50.
Molineux IJ and Panja D. Popping the cork: mechanisms of phage genome ejection. Nat Rev Microbiol 2013;11:194-204.
Moll WD and Guo P. Grouping of Ferritin and Gold Nanoparticles Conjugated to pRNA of the Phage phi29 DNA-packaging motor. J Nanosci and Nanotech (JNN) 2007;7:3257-67.
Moll WD and Guo P. Translocation of Nicked but not Gapped DNA by the Packaging Motor of Bacteriophage phi29. J Mol Biol 2005;351:100-7.
Moncalian G and de la CF. DNA binding properties of protein TrwA, a possible structural variant of the Arc repressor superfamily. Biochim Biophys Acta 2004;1701:15-23.
Morais MC, Koti JS, Bowman VD, Reyes-Aldrete E, Anderson D, and Rossman MG. Defining molecular and domain boundaries in the bacteriophage phi29 DNA packaging motor. Structure 2008;16:1267-74.

Morais MC, Tao Y, Olsen NH, Grimes S, Jardine PJ, Anderson D, Baker TS, and Rossmann MG. Cryoelectron-Microscopy Image Reconstruction of Symmetry Mismatches in Bacteriophage phi29. J Struct Biol 2001;135:38-46.
Mueller-Cajar O, Stotz M, Wendler P, Hartl FU, Bracher A, and Hayer-Hartl M. Structure and function of the AAA+ protein CbbX, a red-type Rubisco activase. Nature 2011;479:194-9.
Niedenzu T, Röleke D, Bains G, Scherzinger E, and Saenger W. Crystal structure of the hexameric replicative helicase RepA of plasmid RSF1010. J Mol Biol 2001;306:479-87.
Niedenzu T, Röleke D, Bains G, Scherzinger E, Saenger W. Crystal structure of the hexameric replicative helicase RepA of plasmid RSF1010. J Mol Biol 2001; 306:479-87.
Olia AS, Prevelige PE, Johnson JE, and Cingolani G. Three-dimensional structure of a viral genome-delivery portal vertex. Nat Struct Mol Biol 2011;18:597-603.
Oram M, Sabanayagam C, and Black LW. Modulation of the Packaging Reaction of Bacteriophage T4 Terminase by DNA Structure. J Mol Biol 2008;381:61-72.
Orlova EV, Gowen B, Droge A, Stiege A, Weise F, Lurz R, van HM, and Tavares P. Structure of a viral DNA gatekeeper at 10 A resolution by cryo-electron microscopy. EMBO J 2003;22:1255-62.
Ortega ME and Catalano CE. Bacteriophage lambda gpNu1 and Escherichia coli IHF proteins cooperatively bind and bend viral DNA: implications for the assembly of a genome-packaging motor. Biochemistry 2006;45:5180-9.
Panja D, Molineux IJ. Dynamics of bacteriophage genome ejection in vitro and in vivo. Phys Biol 2010;7:045006.
Pearson RK, Fox MS. Efects of DNA heterologies on bacteriophage lambda packaging. Genetics 1988;118:5-12.
Pease PJ, Levy O, Cost GJ, Gore J, Ptacin JL, Sherratt D, Bustamante C, and Cozzarelli NR. Sequence-directed DNA translocation by purified FtsK. Science 2005;307:586-90.
Petrov AS and Harvey SC. Packaging double-helical DNA into viral capsids: structures, forces, and energetics. Biophys J 2008;95:497-502.
Petrov AS and Harvey SC. Role of DNA-DNA interactions on the structure and thermodynamics of bacteriophages Lambda and P4. J Struct Biol 2011;174:137-46.
Rafferty JB, Sedelnikova SE, Hargreaves D, Artymiuk PJ, Baker PJ, Sharples GJ, Mahdi AA, Lloyd RG, and Rice DW. Crystal structure of DNA recombination protein RuvA and a model for its binding to the Holliday junction. Science 1996;274:415-21.
Rao VB and Feiss M. The Bacteriophage DNA Packaging Motor. Annu Rev Genet 2008;42:647-81.
Ray K, Sabanayagam CR, Lakowicz JR, and Black LW. DNA crunching by a viral packaging motor: Compression of a procapsid-portal stalled Y-DNA substrate. Virology 2010;398:224-32.
Reddy AB, Gopinathan KP. Presence of random single-strand gaps in mycobacteriophage I3 DNA. Gene 1986;44:227-34.
Sabanayagam CR, Oram M, Lakowicz JR, and Black LW. Viral DNA packaging studied by fluorescence correlation spectroscopy. Biophys J 2007;93:L17-9.
Schwartz C, De-Donatis GM, Fang H, and Guo P. The ATPase of the phi29 DNA-packaging motor is a member of the hexameric AAA+ superfamily. Virology 2013a;443:20-7.
Schwartz C, De-Donatis GM, Zhang H, Fang H, and Guo P. Revolution rather than rotation of AAA+ hexameric phi29 nanomotor for viral dsDNA packaging without coiling. Virology 2013b;443:28-39.
Schwartz C, Fang H, Huang L, and Guo P. Sequential action of ATPase, ATP, ADP, Pi and dsDNA in procapsid-free system to enlighten mechanism in viral dsDNA packaging. Nucleic Acids Res 2012;40:2577-86.
Serwer P. Models of bacteriophage DNA packaging motors. J Struct Biol 2003;141:179-88.
Serwer P. A Hypothesis for Bacteriophage DNA Packaging Motors. Viruses 2010;2:1821-43.
Sharp MD and Pogliano K. Role of cell-specific SpoIIIE assembly in polarity of DNA transfer. Science 2002;295:137-9.
Shu D, Zhang H, Jin J, and Guo P. Counting of six pRNAs of phi29 DNA-packaging motor with customized single molecule dual-view system. EMBO J 2007;26:527-37.
Shu Y, Shu D, Haque F, and Guo P. Fabrication of pRNA nanoparticles to deliver therapeutic RNAs and bioactive compounds into tumor cells. Nat Protoc 2013a;8:1635-59.
Shu Y, Haque F, Shu D, Li W, Zhu Z, Kotb M, Lyubchenko Y, and Guo P. Fabrication of 14 Different RNA Nanoparticles for Specific Tumor Targeting without Accumulation in Normal Organs. RNA 2013b;19:766-77.
Simpson AA, Leiman PG, Tao Y, He Y, Badasso MO, Jardine PJ, Anderson DL, and Rossman MG. Structure determination of the head-tail connector of bacteriophage phi29. Acta Cryst 2001;D57:1260-9.
Simpson AA, Tao Y, Leiman PG, Badasso MO, He Y, Jardine PJ, Olson NH, Morais MC, Grimes S, Anderson DL, Baker TS, and Rossmann MG. Structure of the bacteriophage phi29 DNA packaging motor. Nature 2000;408:745-50.
Singleton MR, Sawaya MR, Ellenberger T, and Wigley DB. Crystal structure of T7 gene 4 ring helicase indicates a mechanism for sequential hydrolysis of nucleotides. Cell 2000;101:589-600.
Sivanathan V, Allen MD, de BC, Baker R, Arciszewska LK, Freund SM, Bycroft M, Lowe J, and Sherratt DJ. The FtsK gamma domain directs oriented DNA translocation by interacting with KOPS. Nat Struct Mol Biol 2006;13:965-72.
Singleton MR, Sawaya MR, Ellenberger T, Wigley DB.Crystal structure of T7 gene 4 ring helicase indicates a mechanism for sequential hydrolysis of nucleotides. Cell 2000; 101:589-600.
Snider J and Houry WA. AAA+ proteins: diversity in function, similarity in structure. Biochemical Society Transactions 2008;36:72-7.
Snider J, Thibault G, and Houry WA. The AAA+ superfamily of functionally diverse proteins. Genome Biol 2008;9:216.
Son M, Hayes SJ, and Serwer P. Concatemerization and packaging of bacteriophage T7 DNA *in vitro*: determination of the concatemers' length and appearance kinetics by use of rotating gell electrophoresis. Virology 1988;162:38-46.
Sun S, Kondabagil K, Draper B, Alam TI, Bowman VD, Zhang Z, Hegde S, Fokine A, Rossmann MG, and Rao VB. The structure of the phage T4 DNA packaging motor suggests a mechanism dependent on electrostatic forces. Cell 2008;135:1251-62.
Sun S, Rao VB, and Rossmann MG. Genome packaging in viruses. Curr Opin Struct Biol 2010;20:114-20.
Sun SY, Kondabagil K, Gentz PM, Rossmann MG, and Rao VB. The structure of the ATPase that powers DNA packaging into bacteriophage T4 procapsids. Mol Cell 2007;25:943-9.
Tang J, Olson N, Jardine PJ, Grimes S, Anderson DL, and Baker TS. DNA poised for release in bacteriophage phi29. Structure 2008; 16:935-43.
Tato I, Matilla I, Arechaga I, Zunzunegui S, de la CF, and Cabezon E. The ATPase activity of the DNA transporter TrwB is modulated by protein TrwA: implications for a common assembly mechanism of DNA translocating motors. J Biol Chem 2007;282:25569-76.
Tato I, Zunzunegui S, de la CF, and Cabezon E. TrwB, the coupling protein involved in DNA transport during bacterial conjugation, is a DNA-dependent ATPase. Proc Natl Acad Sci U S A 2005;102:8156-61.
Thomsen ND and Berger JM. Running in reverse: the structural basis for translocation polarity in hexameric helicases. Cell 2009;139:523-34.
Trottier M and Guo P. Approaches to determine stoichiometry of viral assembly components. J Virol 1997;71:487-94.
Valpuesta JM and Carrascosa J. Structure of viral connectors and their funciton in bacteriophage assembly and DNA packaging. Quart Rev Biophys 1994;27:107-55.
Valpuesta JM, Fujisawa H, Marco S, Carazo JM, and Carrascosa J. Three-dimensional structure of T3 connector purified from overexpressing bacteria. J Mol Biol 1992;224:103-12.
Wang F, Mei Z, Qi Y, Yan C, Hu Q, Wang J, and Shi Y. Structure and mechanism of the hexameric MecA-ClpC molecular machine. Nature 2011;471:331-5.
White JH and Richardson CC. Processing of concatemers of bacteriophage T7 DNA *in vitro*. J Biol Chem 1987;262:8854-60.
Willows RD, Hansson A, Birch D, Al-Karadaghi S, and Hansson M. EM single particle analysis of the ATP-dependent BchI complex of magnesium chelatase: an AAA(+) hexamer. J Struct Biol 2004;146:227-33.
Xiao F, Zhang H, and Guo P. Novel mechanism of hexamer ring assembly in protein/RNA interactions revealed by single molecule imaging. Nucleic Acids Res 2008;36:6620-32.
Xing X and Bell CE. Crystal structures of Escherichia coli RecA in a compressed helical filament. J Mol Biol 2004a;342:1471-85.
Xing X and Bell CE. Crystal structures of Escherichia coli RecA in complex with MgADP and MnAMP-PNP. Biochemistry 2004b;43:16142-52.
Yu J, Moffitt J, Hetherington CL, Bustamante C, and Oster G. Mechanochemistry of a viral DNA packaging motor. J Mol Biol 2010;400:186-203.
Yu XC, Weihe EK, and Margolin W. Role of the C terminus of FtsK in Escherichia coli chromosome segregation. J Bacteriol 1998;180:6424-8.
Zachary A, Black LW. DNA ligase is required for encapsidation of bacteriophage T4 DNA. J Mol Biol 1981;149:641-58.
Zachary A, Black LW. Topoisomerase II and other DNA-delay and DNA-arrest mutations impair bacteriophage T4 DNA packaging *in vivo* and *in vitro*. J Virol 1986;60:97-104.
Zhang F, Lemieux S, Wu X, St.-Arnaud S, McMurray CT, Major F, and Anderson D. Function of hexameric RNA in packaging of bacteriophage phi29 DNA in vitro. Mol Cell 1998;2:141-7.
Zhang H, Schwartz C, De Donatis GM, and Guo P. "Push Through One-Way Valve" Mechanism of Viral DNA Packaging. Adv Virus Res 2012;83:415-65.
Zhang H, Endrizzi JA, Shu Y, Haque F, Sauter C, Shlyakhtenko LS, Lyubchenko Y, Guo P, and Chi YI. Crystal Structure of 3WJ Core Revealing Divalent Ion-promoted Thermostability and Assembly of the Phi29 Hexameric Motor pRNA. RNA 2013;19:1226-37.
Zhang Z, Greene B, Thuman-Commike PA, Jakana J, Prevelige PE, Jr., King J, and Chiu W. Visualization of the maturation transition in bacteriophage P22 by electron cryomicroscopy. J Mol Biol 2000;297:615-26.
Zhao Z, Khisamutdinov E, Schwartz C, and Guo P. Mechanism of One-Way Traffic of Hexameric Phi29 DNA Packaging Motor with Four Electropositive Relaying Layers Facilitating Anti-chiral Revolution. ACS Nano 2013;7:4082-92.